Addis Ababa University

Addis Ababa Institute of Technology

School of Electrical and Computer Engineering

Control of lower limb exoskeleton with simulated EMG signal

A Thesis Submitted to the School of Graduate Studies of Addis Ababa University in Partial Fulfillment of the Requirements for the Degree of Masters of Science in control Engineering

By Bethlehem Aberra

Advisor: Dr. Mengesha Mamo

Co-advisor: Mr. Andinet Negash

April 2016

Addis Ababa, Ethiopia

Addis Ababa University
Addis Ababa Institute of Technology
School of Electrical and Computer Engineering

Control of lower limb exoskeleton with simulated EMG signal

By Bethlehem Aberra

Approval by Board of Examiners

______________________	_______________
Dean, School of Electrical And Computer Engineering	Signature
Dr. Mengesha Mamo Advisor	_______________ Signature
Mr. Andinet Negash Co-Advisor	_______________ Signature
Dr. Dereje Shiferaw External Examiner	_______________ Signature
Mr. Getu Gabissa Internal Examiner	_______________ Signature

Declaration

I, the undersigned, declare that this thesis work, to the best of my knowledge and belief, is my original work, has not been presented for a degree in this or any other universities, and all sources of materials used for the thesis work have been fully acknowledged.

Name: Bethlehem Aberra Signature: ________________

Place: Addis Ababa

Date of submission: April 18, 2016

This thesis has been submitted for examination with my approval as a university advisor.

Dr. Mengesha Mamo ____________________
Advisor Name Signature

Mr. Andinet Negash ____________________
Advisor Name Signature

Acknowledgment

First and foremost, I would like to thank God for his blessing and grace. Secondly, my deep gratitude goes to my thesis advisor, Dr. Mengesha Mamo and co advisor Mr. Andinet Negash, for their valuable comments, suggestion and guidance which helped me a lot in pursuing through my thesis work. Besides the comments, suggestion and guidance Dr. Mengesha and Mr. Andinet their commitment in arranging a monthly progress report time was undeniably so helpful. In particular I am grateful to Mr. Andinet for enlightening me the first glance of my thesis.

I am deeply indebted to my postgraduate classmates, undergraduate students who worked with me, and colleagues, especially Mr. Amdail Shifaw, who helped me to sort things out when we discussed topics that occupied my mind.

My grateful appreciation goes to my best friends and Mr. Tewodros shigute for always believing in me, motivating, and suggesting ideas in the course of my MSc study and thesis work.

My parents Mr. Aberra Sufa and Mrs. Mulunesh Degu deserve a special thanks in ways too numerous to mention.

Finally, last but certainly not least, I want to express my grateful appreciation to my husband, Tekalign, for his love, support, encouragement, and everything else during those times when I needed it most. There are so many others whom I may have unintentionally left out and I sincerely thank all of them for their help.

Abstract

An exoskeleton robot is a kind of a man-machine system which mostly uses combination of human intelligence and machine power. The structure of an exoskeleton robot consists of joints and links which correspond to the human body.

This thesis presents a control system for exoskeletons that utilizes the simulated electrical signals from the muscles, EMG signals, as the main means of information transportation between the human and the exoskeleton. A support action is computed in accordance to the patient's intention and is executed by the exoskeleton. The mathematical model of the exoskeleton system was based on the mathematical model of a permanent magnet DC servo motor whose parameters can be selected by either Using system identification techniques on a prototype built or by selecting an actuator based on the requirement of the load torque. A linear quadratic Gaussian (LQG) controller for the lower-limb exoskeleton is designed and implemented. Furthermore the robustness of the system to sensor noise and unmodelled system dynamics were analyzed.

The effectiveness of the proposed system is tested through simulation studies using Simulink® software. The 3-D model of the system designed using solidworks® is interfaced with the Simulink® model via Simulink® simmechanics product. The proposed control strategy has shown satisfactory performances in terms robustness and gentleness. The knee joint is to track the ideal range of motion with an error of less than 5 % with the use of LQG controller. The control law is also found to be robust with respect to external disturbances.

Key words: Lower limb exoskeleton, Electromyography (EMG), Modeling, linear quadratic Gaussian (LQG) controller.

Table of Contents

List of Figures

List of Tables

List of Acronyms

ALEX	Active Leg Exoskeleton
BLEEX	Berkeley Lower Extremity Exoskeleton
DC	Direct Current
DOF	Degree Of Freedom
EMG	Electromyography
GRF	Ground Reaction Force
HAL	Hybrid Assistive Leg
HULC	Human Universal Load Carrier
LEE	Lower Extremity Exoskeleton
LOPES	Lower Extremity Powered Exoskeleton
LQG	Linear Quadratic Gaussian
LQR	Linear Quadratic Regulator
MIT	Massachusetts Institute Of Technology
PID	Proportional, Integrator And Derivative
POGO	Pneumatically Operated Gait Orthosis
RAGT	Robot-Assisted Gait Training
SCI	Spinal Cord Injury
SUBAR	Sogang University Biomedical Assistive Robot
ZMP	Zero Moment Point
3D	Three Dimensional

Chapter 1. Introduction

1.1. Background

According to the data from Cheshire services Ethiopia, there are over six million people who are disabled in Ethiopia, representing 7.6% of the total population. Of these, at least 44% result in paraplegia [42]. One of the most significant impairments resulting from paraplegia is the loss of mobility, particularly gives the relatively young (average) age at which such injuries occur. Surveys of persons with paraplegia indicate that mobility concerns are among the most prevalent, and that chief among mobility desires is the ability to walk and stand. In addition to impaired mobility, the inability to stand and walk entails severe physiological effects, including muscular atrophy, loss of bone mineral content, frequent skin breakdown problems, increased incidence of urinary tract infection, muscle spasticity, impaired lymphatic and vascular circulation, impaired digestive operation, and reduced respiratory and cardiovascular capacities[1].

The outcomes of rehabilitation therapy that implements body weight support treadmill training for incomplete spinal cord injuries (SCIs) and stroke patients have been reported in several previous studies since the 1990s. SCI involves damage to any component of the nerves or spinal cord located at the end of the spinal canal, which is either complete or incomplete. However, it often causes permanent changes in strength, sensation and other body functions below the site of the injury. Furthermore, the loss of motor control prevents a patient from performing a precise movement in coordination with the timing and intensity of the muscle action [6]. The orthosis is done by manual training, operating the patient's paralyzed legs physically by two therapists Traditional rehabilitation therapies are very labor intensive especially for gait rehabilitation, often requiring more than three therapists together to assist manually the legs and torso of the patient to perform training [43]. This fact imposes an enormous economic burden to any country's health care system thus limiting its clinical acceptance. Furthermore, demographic change (aging), expected shortages of health care personnel, and the need for even higher quality care predict an increase in the average cost from first stroke to death in the future. All these factors stimulate innovation in the domain of rehabilitation in such way it becomes more affordable and available for more patients and for a longer period of time [4]. A good and promising solution for this is the use of robots for rehabilitation.

Robotics for rehabilitation treatment is an emerging field which is expected to grow as a solution to automate training. Robotic rehabilitation can (i) replace the physical training effort of a therapist, allowing more intensive repetitive motions and delivering therapy at a reasonable cost, and (ii) assess quantitatively the level of motor recovery by measuring force and movement patterns.

An exoskeleton robot is kind of a man-machine system which mostly uses combination of human intelligence and machine power. Besides mentioning in early patents and science fiction, research in powered human exoskeleton devices began in the late 1960s, almost in parallel between a number of research groups in the United States and in the former Yugoslavia. However, the former was primarily focused on developing technologies to augment the abilities of able-bodied humans, often for military purposes, while the latter was intent on developing assistive technologies for physically challenged persons [1]. Important scientific research started in the 1970's where the group around Vukobratovic played a pioneer role: They had a clear goal in mind to help patients with defects in their loco motor system to regain walking capabilities. At this time, lack of computer processor power, heavy actuators (both pneumatic and electrical), and heavy power supplies limited the realization of interesting theoretical results. Skin surface electromyogram (EMG), which is one of the biological signals, is often used in order to control the robot according to the user's intention since it directly reflects the user's muscle activity level in real time [4].

Nowadays orthosis assistive robots such us the driven gait orthosis (DGO), also known as LOKOMAT, LOPES (Lower extremity Powered ExoSkeleton), a robot-assisted gait training (RAGT) with an active leg exoskeleton (ALEX), also integrating the AAN rehabilitation strategy into the orthosis system, LOKOIRAN are designed to be suitable for patients with various diagnoses, such as SCI, stroke, multiple sclerosis (MS) and sport injury cases, aging and people with balance and locomotion disorders [6].

1.2. Problem description

In designing an exoskeleton not only the mechanical part is an important field of research but also the control method is an important area of research. If a light weight and powerful exoskeleton existed, there still remains the problem of how to control the device. The interface between the operator and the exoskeleton is as important as the mechanical construction.

The robot can perform the effective power assist if the motion intention of the user is precisely estimated based on the EMG signals in real time. However, realizing the precise EMG signals is not used in my case the simulated EMG signal is used. Since misinterpretation of the desired movement of the operator can lead to injuries or worse, the control mechanism should somehow be robust, i.e. maintains system response and error signals within prescribed tolerances despite the effects of uncertainty on the system, and gentle: meaning that movements have to be smooth and safe. Considering these criterions a Linear Quadratic Gaussian (LQG) controller is utilized. In designing the LQG two main blocks, the Kalman estimator and linear quadratic regulator, are designed. The Kalman state estimator is designed to estimate the states (armature current, angular position, and angular velocity) and then using the estimated states the optimal control law is obtained by multiplying it with the state feedback gain used in the LQR control system. Therefore in this research work, the control of a lower limb exoskeleton actuated only at the knee is done using an LQG controller with simulated EMG signal as a reference input.

1.3. Objectives

1.3.1. General objectives

The main objective of this research is to design and implement a lower-limb exoskeleton controller; which is gentle, affordable, and moreover robust to the effect of modeling errors and disturbance.

1.3.2. Specific objectives

The specific objectives of this thesis are:

- To study and understand the general background of the exoskeleton.
- To study the currently utilized rehabilitation therapy in Ethiopia.
- To mathematically model and analyze the exoskeleton system.

- To model the system and the dynamic behavior into a working simulation in order to design the controller.
- To Design a gentle and robust control system for the knee of the exoskeleton.
  - To design the kalman state estimator.
  - To design a linear quadratic regulator/obtaining the optimal state feedback gain.
- To test the overall system through simulation studies using Simulink.
- To draw conclusion based on the analysis of results obtained from simulation studies of the proposed control system and to provide recommendations for improvement.

1.4. Motivation, contribution and Scope of the Thesis

Thousands of Ethiopians lose limbs every year as a result of war, violence, industrial accidents, and unfound land mines. The only rehabilitation center in the country, i.e. the Menagesha rehabilitation center under the Cheshire services Ethiopia, give it's patients a manual rehabilitation therapy which puts the efficiency of the therapy given in question. Hence the work from this thesis will provide an automatic rehabilitation, which owes a great support for both the patient and care provider.

In designing the lower limb exoskeleton for the automatic rehabilitation proposed the mathematical and 3-D model for the system is developed first and Linear Quadratic Gaussian Controller is designed to provide a robust control over the knee joint.

The outcome of this research is based on the simulation of the proposed techniques using a MATLAB/ Simulink® simulation tool.

1.5. Outline of the thesis

Chapter 1

Presents the background of the Exoskeleton system, problem statement and the objective as well as the motivation, contribution, and scope of the thesis.

Chapter 2

The literature review of previously done researches and the classification of control methods on lower extremity exoskeleton is presented here.

Chapter 3

In this chapter the Exoskeleton system and the overall thesis methodology followed is discussed. The brief introduction to an exoskeleton system, actuator selection for the system, the two approaches for obtaining a mathematical model, and the selected 3-D model of the system are presented. The methodology of obtaining the simulated EMG signal and finally the controller design is thoroughly discussed.

Chapter 4

Is dedicated to show simulation setups, simulation results, and discussion of the obtained result.

Chapter 5

Conclusions, recommendations and suggestions for future work are all presented in this chapter.

Chapter 2. Literature review

Over the last decade, there has been a significant increase in the research and development of exoskeleton devices across the globe. An exoskeleton is defined as an actuated device with an anthropomorphic configuration which could be attached externally to the limbs. They are typically designed to provide interaction forces that assist the user, be it for rehabilitation or for strength augmentation purposes.

Since the thesis only focuses on the lower extremities, this chapter will present the background information and a brief review of the works done in the field of lower extremities exoskeleton research. In terms of hardware, they can be classified according to the portability of the device, with each device being either portable or non-portable. A comprehensive survey on portable lower-extremity exoskeletons and active orthoses was done in [25]. The following review serves to supplement with an updated survey in the field of portable lower-extremity exoskeletons as well as to familiarize in the development of non-portable lower-extremity exoskeletons which are mainly used in gait rehabilitation. The list is not exhaustive, for the number of assistive robots for lower extremities has grown exponentially over the last few years. And this review will only focus on the more prominent developments in the field.

The last section will attempt to classify and discuss the feasibility of the various control strategies employed on these devices for our purpose.

2.1. Lower Extremity Exoskeleton Research

2.1.1. Rehabilitation or Mobility

This category of exoskeleton is designed to aid patients with lower extremity paralysis or weakness due to spinal cord injury (SCI) or neurological disease in their daily locomotion activities. While others are primarily developed for automated gait training on a treadmill for rehabilitative purposes.

Figure 2.1 : Non-portable exoskeleton for gait training, namely ALEX (left), Lokomat by Hocoma (Centre), and LOPES by Uni. Of Twente (Right)

Lower limb exoskeletons for rehabilitation (Fig. 2.1) are often non-portable devices combined with a treadmill and a body-weight support system for automated gait training. These devices are designed to allow severely impaired patients to engage in gait therapy. Some of the commercially available devices for this non-portable class of exoskeleton are the Lokomat and Autoambulator. Others devices developed for research include the ALEX (Active Leg EXoskeleton) , POGO (Pneumatically Operated Gait Orthosis) [24] and LOPES (Lower Extremity Powered Exoskeleton) [23]. These devices will be reviewed shortly with the exception of the Autoambulator as no scientific publication could be found on this device as far as I have reviewed. The Lokomat, developed by Hocoma, consist of a body weight support system with an exoskeleton with actuation at the hip and knee joints in the sagittal plane. The ankles are held up by passive straps to prevent them from hitting the ground during swing. During gait training, the patient is generally made to follow a predetermined gait trajectory repetitively. Thus, in earlier version of Lokomat, the patient limbs are forced to strictly follow the predetermined path under position control and the human will have little influence over the trajectory of the exoskeleton. However, a robot driven patient will not experience cycle-to-cycle variation in the kinematics and sensorimotor feedback. This may cause habituation to sensory input, reduce sensory responses to weight-bearing locomotion and ultimately impair motor learning [22]. Therefore, newer generation of Lokomat, and other rehabilitation robots, aim to achieve an Assist-As-Needed (AAN) system. Later generations of Lokomat implemented impedance control [21], in order to realize an AAN control scheme. It is done with the help of multiple force sensors at user attachment points to detect the interaction forces between the user and the Lokomat.

The ALEX is developed by the University of Delaware. ALEX's hardware closely resembles that of the Lokomat, with the exception of force sensor at every actuated joint for the ALEX. This enables the ALEX to perform force control at the joint level. To achieve the ANN paradigm, it utilizes a force field method to create the virtual tunnel to guide the patient's gait trajectory to follow a predetermined gait pattern rather than enforcing the patient to strictly follow the path. This 'softer' approach encourages more patient cooperation during rehabilitation, and improvement have been observed in stroke patients who had participated in their gait training studies [26].

The major difference of the POGO and LOPES as compared to the Lokomat and ALEX is that they incorporated compliant actuators into their joint design with low intrinsic impedance in order to enhance their force tracking performance and safety in human-robot interaction. In the modulation of the robot's impedance using feedback from force sensors, there is a limit to the amount of inertia reduction which can be achieved without the risk of coupled instability. The residual inertia may create large interaction forces between the human and the robot which will affect dynamic gait motion. The POGO utilizes pneumatic actuators to actuate the hip and knee in flexion and extension. On the other hand, the LOPES uses Series Elastic Actuators (SEA), a concept first introduced in [20], to enhance back-drivability of the system whereby the desired impedance of the system is set to zero for the subject to move with minimal hindrance from the robot. Electromyography (EMG) measurements of a subject on eight leg muscles showed that free walking in the LOPES closely resembles that of free treadmill walking. This indicates that the impedance of the LOPES is sufficiently low to not adversely change the gait pattern of an individual attached to the device.

Figure 2.2: From Left to right, ReWalk by Argo Medical technologiesl; Esko by Berkeley Bionics; REX by Rexbionics ; and SUBAR by the University of Sogang

Lower limb exoskeleton for mobility (Fig. 2.2) is generally built to aid disabled patients or those suffering from general weakness, namely paraplegics and the elderly, to go about and perform their daily walking activities.

The main objective of the Rewalk [19] developed by Argo Medical Technologies, Israel, , the Vanderbilt exoskeleton [18] by Vanderbilt University, USA and the Esko by Berkeley Bionics which is now known as Esko Bionics, USA, is to enable paraplegic users to walk again. The user balances through the use of crutches. Using an array of the sensors information from the exoskeleton itself and the crutches, the device estimates the user's intention and executes the gait pattern stored for the particular mode of operation (such as walking, stairs-climbing and sitting). However, the method of user's intention detection is not known to the public since they are commercial products. Rewalk uses highly geared DC motors to actuate the hip and the knee joints, while ESKO uses hydraulic actuation on similar joints.

REX [17] developed by Rexbonics in New Zealand, allows the paraplegic user to stand and walk without the use of crutches or other supports. User commands the motion of the exoskeleton using a joystick, and REX executes a gait trajectory in that direction. A balancing algorithm ensures that the device and the patient remain stable during the entire motion. However, as it is a commercial device, the method of balancing is not made public.

The SUBAR (Sogang University Biomedical Assistive Robot) [26] developed by the University of Sogang, South Korea, is designed for assisting people with severe impairments. It uses a rotary SEA to generate sufficiently high torque at low levels of impedance. It has exhibited good force tracking performance, but higher level algorithms to determine assistive torques are still under development as of 2013.

2.1.2. Strength Augmentation

This class of exoskeletons is commonly portable device which assists the user by augmenting the joint torque and work to complete a specific task, e.g. stairs ascend. They can be used with patients with weaken legs, like the elderly, or on healthy individuals to increase their performance in terms of strength or stamina.

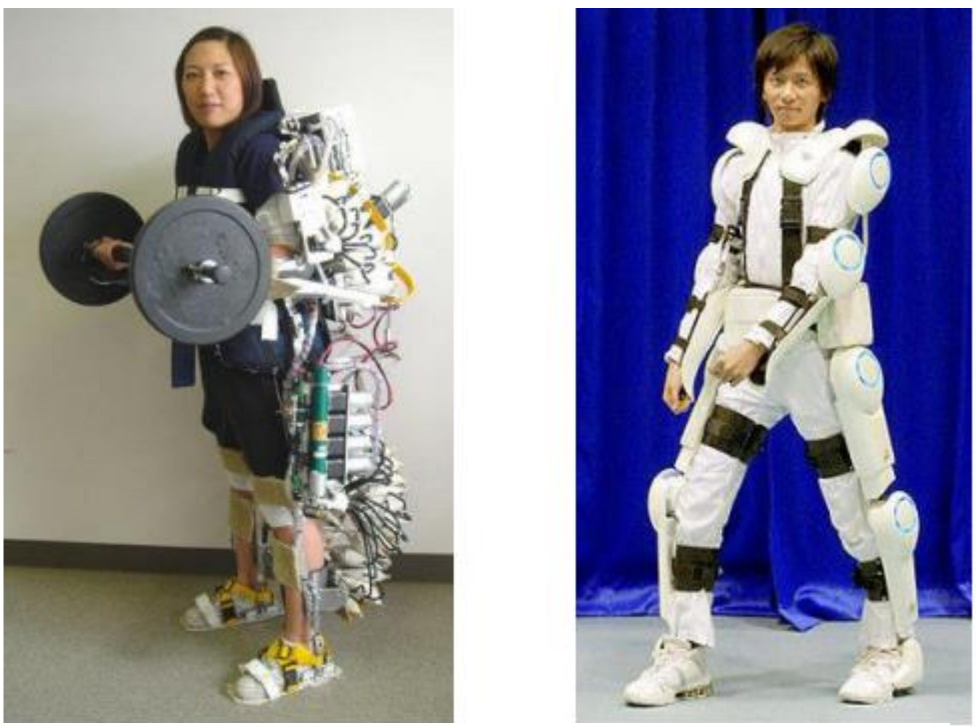

Figure 2.3: Power Assist Suit developed by the Kanagawa Institute of Technology (left) and HAL 5 by Cyberdyne (right)

One such exoskeleton design is the Power Assist Suit (Fig. 2.3) developed by the Kanagawa Institute of Technology. It is developed to aid nursing personnel in carrying patients by providing assistive torque at the elbow, waist and knee joints. The user intended torque is measured by a novel muscle hardness sensor. The assistive torque is derived from the intended torque, which is then given to the joint by regulating the pressure of the pneumatic actuators [26].

The Hybrid Assistive Leg (HAL) jointly developed by the University of Tsukuba and Cyber dyne (Fig. 2.4) to aid elderly or weaken patient to walk. It has also demonstrated the capability to increase the strength of an abled-body individual. The HAL uses DC motor with harmonic drive to power the movement of the hip and knee joints. For control, the HAL system uses skin-surface electromyography (EMG) signals and joint encoders to determine the intended user’s torque. The EMG readings of the antagonistic muscles across a joint and the kinematic information of the user’s limb are fed into a muscle model of the particular user to generate the estimated torque. Parameters of the muscle model have to be predetermined over multiple trials which would take extended period of time. Hence, HAL reportedly needs two months to be optimally calibrated for an individual. In the recent years, some research efforts towards intent based detection using the user’s kinetic and kinematic information have been made. HAL utilizes a phase sequence approach which assumes sequential motion of the user and infers the transition to the next motion state based on joint angles and ground reaction force (GRF) information [16]. They have shown it effectiveness in sit-to-stand and stand-to-sit transfers [16], and in supporting walking. However, transition between walking motion to other motion states is not addressed. Current developments of the HAL are not made public due to the commercialization of HAL-5.

The Lower Extremity Exoskeleton (LEE) from Nanyang Technological University, Singapore, is designed to aid soldiers in load carrying (Fig. 2.5). The LEE uses position controller DC motors for actuation. To track the trajectory of the user, the exoskeleton utilizes a master and slave type of control which is traditionally used in tele-robotics. An inner exoskeleton equipped with encoders will capture the joint information of the user and feedback the command position to the actuators of the outer exoskeleton [26].

To ensure that the exoskeleton can remain stable, a zero-moment point (ZMP) controller is applied to provide postural stability. This is achieved by shifting the position of the trunk in order to change the position of the ZMP of the exoskeleton such that the combined ZMP of the human and exoskeleton system remains within the support polygon.

Figure 2.4: The Lower Extremity Exoskeleton (LEE) (left) and Under-actuated exoskeleton with passive elements (right)

MIT Bio mechatronics labs developed an under-actuated quasi-passive exoskeleton that supports the weight of the payload (Fig. 2.4). It utilizes elastic spring at the hip and ankle joints to store energy during negative work phase of the gait and releases the stored energy during the positive work phase of the gait [26]. In addition, a variable damper at the knee joint is controlled to dissipate energy at appropriate times during level walking. During operation, this system reportedly consumes only 2W of power input which is mainly used for the control of the variable damper. Later version includes an actuated hip joint to actively assist in leg swing. The control of this device is achieved by detecting the phase of the gait by means of joint sensors and ground reaction force sensors, before appropriate assistive action is applied at each joint.

Figure 2.5: XOS 1 (left) and XOS 2 (right)

The XOS developed by Raytheon Sarcos, USA, is a full body pseudo anthropomorphic exoskeleton, designed to increase human strength and load carrying capability of a soldier (Fig. 2.5). It uses rotary force controlled hydraulic actuators to power each joints and load cells as force sensors at the end effectors [15]. It has been shown that an individual can carry a 90 kg load with ease while wearing the XOS. In a later version, the XOS 2, energy efficiency of the device was improved by 50% with a help of a dual pressure system. The exoskeleton controller aims to track the actuator output force to the measured human-robot interaction force by a force amplification factor. It has shown that through this force-based feedback control, a scaled version of the effective mass, disturbance and viscous forces can be felt by the user, depending on the force amplification factor.

Figure 2.6: BLEEX by University of California (left) and HULC by Berkeley Bionics (right)

The Berkeley Lower Extremity Exoskeleton (BLEEX) developed by University of California, Berkeley, is designed to increase human weight carrying capability (Fig. 2.6). The system is actuated by force controlled linear hydraulic pistons [14]. Berkeley Bionics was setup as a spinoff company to further develop BLEEX. The same company is also involved in the development of the Esko mentioned earlier. Its latest exoskeleton, the Human Universal Load Carrier (HULC) is able to carry 200 Ibs over an extended period of time. To control the device, an inverse dynamics model of the system is used to calculate the human-robot interaction force. With the interaction force, the controller, similar to the XOS's, will attempt to track the actuator output force to the measured human-robot interaction force by a force amplification factor, thereby increasing the sensitivity of the robot link. The main advantage of the BLEEX method of control over the XOS is that the user can interact with any arbitrary part of the link, thereby increasing the maneuverability of the user. However, this method is not without its disadvantages. Being heavily model based means a relatively accurate dynamic model of the system is needed for control.

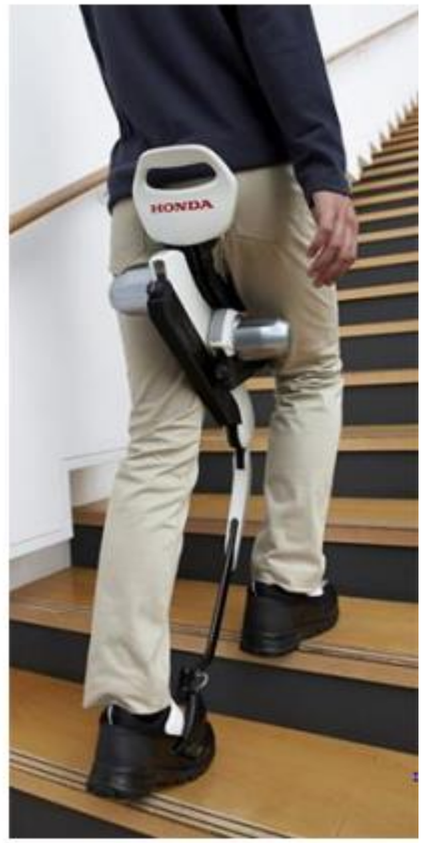

Figure2.7: Honda's Stride Management Assist Device (left) and Walking Assistance Device (right)

Recently, Honda had developed two devices aimed to aid elderly in walking. It was reported that they could be used by healthy individuals to increase their endurance in prolong walking or squatting task as well. They are namely the stride management assist device and the walking assistance device as shown in Fig 2.7.

The stride management assist device [13] is designed to assist the user in hip flexion and extension during walking. This helps to lengthen stride length, hence making it easier for the user to cover a longer distance within a given time. It is light weight device designed to be worn at the hips of the user. The assistive force provided by two brushless DC motor at each side of the hip is controlled by a network of adaptive oscillators that entrains to the user's gait frequency. The complex network of oscillators is required to minimize undesirable interaction forces during synchronization, and maximize assistance force once synchronization is achieved.

The walking assistance device [12] is designed to relieve the load on the user's legs to reduce physical exertion and fatigue. It is only actuated at the knee joints and a special mechanism helps maintain the stability of the sit during motion. According to their patent [11], the lifting force of each leg of the device is controlled such that the sum of both supporting force, measured by a load cell at each link, is equal to a pre-defined target lifting force. It has demonstrated capability in assisting walking, crouching and stairs ascending of the user.

2.2. Classification of Control Methods

From the review of lower extremity exoskeleton research in the previous section, one could see the wide diversity in designs and control methods used. Several of the exoskeleton systems are commercialized products; hence their detailed method of control and effectiveness remains unknown to the literature.

Given that we are interested in designing a control method that will provide the user with intuitive assistance in ADLs and gait rehabilitation process, a detail survey of the existing control strategies and an evaluation of how they might benefit our device needs to be done. Results of control methods employed in upper arm rehabilitation robotics and other passive or simple leg orthosis device will also be looked into for their valuable insights.

A possible method of classification of the control methods for these devices could be based on the level of motion autonomy it provides the user as shown in Fig 2.8. Autonomy in this context is defined as the ability of the user to control the movement of the exoskeleton device. On one end of the spectrum, we have full autonomy which means that the motion of the system is entirely driven by the user. While on the other end of the spectrum, we have no autonomy which means that the motion of the system is entirely device driven and the user will have no influence on its motion.

Figure 2.8: Control method depending on the level of autonomy in the system

2.2.1. Force Amplification

Robotic force control is a well-studied field which aims to maintain a constant force level between a robot and the environment. When applied to an exoskeleton, the goal of the controller is to maintain minimal interaction force between the robot and the user. It is utilized by the XOS, BLEEX and HULC. In this way, the mechanical impedance of the robot is minimize from the point of view of the user [26]. As the result, the device shadows the movement of the user such that the user feels minimum hindrance.

This type of control provides the user with full autonomy in motion. However, it assumes the user is capable of performing the intended motion and merely tracks the motion. From the point of view of the user, the device does not assist his free motion. The assistance is only felt in the form of reduced effort in carrying or manipulating an external object.

As it lacks the ability to provide assistance in free motion, this control method is deemed to be unsuitable for assisting a stroke patient in rehabilitation or ADLs.

2.2.2. Master and Slave

Master and slave control is traditionally used in tele-robotics [10] to mimic the movement of the operator. In the case of LEE and the Hardiman [9], the exoskeleton is controlled to track the position of the user which is measured via a wearable motion capture system. Position tracking could be performed in the joint space or operation space. Nonetheless, similar to the force amplification approach, this configuration assumes the user is capable of performing the intended motion without assistance.

While it may seem that this method of control may not be suitable for our purpose, master and slave control method has been prevalent in upper limb rehabilitation, in the form of motion mirroring [26], with promising results.

However, for application to lower limb devices, the mirroring process will have to be more complex than direct one to one mirroring [26]. A higher-level supervisory controller is required to recognize if the current motion requires lower limbs movement to be in phase or in anti-phase.

2.2.3. Gravity Compensation

In robotics, gravity compensation is a method by which the gravity loading on each joint of the robot is calculated and the torque at each joint is controlled to account for these effects. When applied to an exoskeleton system, this control method attempts to nullify the effects of gravity on the user, thus relieving the user the effort to work against the gravity. Usually, gravity compensation is done in the form of either a body weight support or a limb support as discussed below.

Body weight support is commonly achieved with the user being mechanically supported by a harness that is linked to a counter-balance weight via a rope [8]. The Honda's walking assistance device mentioned in the previous section provides gravity assisting force on the body in a compact design. This relieves the legs of a portion of load bearing during stance phase for say stairs ascending.

For limb support, passive gravity-balanced device for upper limb rehabilitation, such as the WREX [26], have shown that it could benefit patients in motor learning capability. Inspired by the results from upper limb rehabilitation, Banala et al. [29] had developed a passive lower limb orthotic device which is able to negate the effects of gravity during swing phase. They are able to show reduce muscle effort in static position task and increase range of motion at the hip and knee joints of a stroke patient.

Since no desired trajectory is enforced on the user, gravity compensation allows the user to have full autonomy. The user can move freely under his control, while the device merely provides necessary assistive force to partially or completely negate the effects of gravity on the user. This form of assistance is reasonable in upper limb tasks, such as pick and place, where alleviating the arms gravitational burden allows point to point movement in ones' workspace with less effort. However, gravity plays an important in the pendular exchange of energy during human walking [26]. The human gait exploits the effects of gravity in some parts of the gait, for example during limb deceleration before heel strike. Hence, a sole gravity balancing controller may not be suitable to assist the entire gait cycle.

2.2.4. EMG based

There are two main types of EMG based controllers, namely using EMG for direct amplification and using EMG as a motion initiation. In direct amplification, EMG signal is used to predict intended joint torque of the user. It offers the user full control of the device since the user can control each joint as long as a relationship between the major muscles and joint of interest is established. Moreover, it is able to predict motion intent and provide the necessary assistive torque before the actual motion. Thus, it is attractive to stroke or weaken patients who do not have the capability to move without assistance.

However, this method is not without its drawbacks. Firstly, acquiring the relationship between joint torque and EMG signal is non-trivial. To get an accurate estimate of joint torque, all major muscles that involved in the joint motion needs to be taken into account. While some muscles are superficial, some muscles are deeper, requiring the need of intra-muscular electrodes. In addition, moment arms of each muscle and its variation with flexion angle will have to be determined. Furthermore, EMG signals do not reveal of the torque contributed by the passive elements of the muscle, so a mechanical muscle model is required for every involved muscle [28]. Lastly, the noisy and time-varying nature of the EMG signals makes signal conditioning task difficult. In [27], developers of HAL find this method of control to be uncomfortable to the user.

The use of EMG as motion initiation usually involves the monitoring of muscle activity to a predetermined threshold level. A predetermined motion or assistive force will be executed once the threshold condition is met. It offers less autonomy as compared to the previous EMG based method, since the user will have little or no control over the prescribed task once it is triggered. However, it is simple and achieves the objective of increasing patient involvement during training. In upper arm rehabilitation, significant reduction in arm spasticity is observed with patient under EMG triggered robot assistance [26]. Spasticity is a neurological condition causing an abnormal increase in muscle tone due to excessive contraction of the muscles that occurs when the muscle is stretched. Excessive spasticity limits the frequency and intensity of rehabilitative exercises that could be administered.

2.2.5. Phase of Gait

This control method employs a mean to estimate the intended motion of the user based on the sensor data. It aims to inject an appropriate amount of force in the correct direction that will be assistive to the user during that particular phase of motion. The Honda's stride management assist, HAL and MIT's exoskeleton are examples of systems using this class of controller. Some uses adaptive oscillators, while others utilize kinematic thresholds to achieve a synchronized assistive force. The user may not have full autonomy over the system as their limbs are forced by the device to complete a predefined gait sub-task. However, some autonomy comes in the form of self-initiated motion.

HAL utilizes a phase sequence approach which assumes sequential motion of the user and infers the transition to the next motion state based on joint angles and ground reaction force (GRF) information [16]. They have shown to lower muscle activations of the knee flexors during sit-to-stand and stand-to-sit transfers [16], and the hip flexors and extenders during walking. Similarly, MIT's exoskeleton addresses a level walking task. However, transition between walking motion to other motion states is not addressed. Hence, autonomy of user motion is limited to within the predefined motion state.

Commercial lower limb exoskeletons for mobility have shown their effectiveness in assisting paraplegics to perform daily locomotion task. From demonstrations, they are able to detect the motion intention of the user and aid the user in the desired motion task. However, the techniques involved are not disclosed in the literature.

2.2.6. Manual Control

An example of a manual control scheme would be the REX. A joystick at the side of the arm allows the user to control the movement of the REX and to switch to other motion modes. Johnson et al. [7] proposed an interesting approach of manual control by tracking a corresponding finger joint angle to a corresponding leg joint angle. However, manual control method is still not intuitive and requires constant conscious control by the user.

2.2.7. Others

Fixed trajectory controller, like the earlier versions of Lokomat and Autoambulator, are positioned control to move the user's limb over a predetermined gait trajectory. They offer the least amount of autonomy since user participation is disregarded. In comparison, compliant trajectory, like LOPES and Lokomat, offers the user a little more autonomy in motion as some error in joint kinematics is tolerated.

Haptic guidance, like the ALEX, provides a force field about a predetermined gait trajectory. The user has the choice to initiate movement, but the gait trajectory is confined within a virtual tunnel.

The controllers mention in this section offer little autonomy. However, they are often embedded within a sub-motion state in conjunction with controllers in previous sections.

2.3. Summary

In this chapter, we gave an overview of lower extremity exoskeleton research in a range of applications. The advantages and disadvantages of several types of control methods are also discussed. Besides the classification of control methods based on the level of autonomy as stated in section 2.2 the control method can be classified based on the controller/ control system different researchers have used in their work. The hierarchical neuro-fuzzy controller, classical controllers (i.e. PID and P), Inverse control and loop transfer recovery (LTR) feedback control, Adaptive impedance control using boundary-layer-augmented sliding mode control (BASMC) can be listed among the utilized controllers which shows most of the researchers did not consider the need for robustness. Additionally current commercialized exoskeleton systems are very costy and out of reach to make use of them in developing countries like Ethiopia.

Chapter 3. The Exoskeleton system and Methodology

3.1. The Exoskeleton system

3.1.1. Introduction

The concept of exoskeleton is emerging from biology. Some creatures like turtles and crabs have external structure called exoskeleton, which provides safety from environment and other animals, sensory medium for outside world, attachment for muscles etc.

An exoskeleton robot is kind of a man-machine system which mostly uses combination of human intelligence and machine power. The structure of an exoskeleton robot consists of joints and links which are corresponding to the human body. These robots are used to transmit the torque from the actuators to generate the motion. These robotic systems are used for different applications such as rehabilitation, human power amplification, motion assistance, virtual reality etc. Exoskeleton robots can be classified according to the place where it supports the human body. This includes upper extremity, lower extremity and full body [2].

The upper limb or upper extremity is the region in an animal extending from the deltoid region to the hand, including the arm, axilla and shoulder. Lower extremity or limb of the human body includes the foot, thigh and even the hip or gluteal region [42].

Design of exoskeleton robots are not straight forward and it needs lot of factors into consideration. The special features of the human anatomy should be considered in order to produce user friendly exoskeleton system. Obtaining exact human motion from exoskeleton robot is still a challenge for the researches in this field [2].

The control systems of the exoskeleton robots are completely differ from the traditional robots [3]. This is because the human operator is not only the commander or the supervisor of the system but also a part of the control loop in these control systems. Hence, it is known as 'man-in-the loop' [1]. The human operator mainly makes the decisions and the exoskeleton implements the tasks. However, feedback information received by the human operator and the exoskeleton robot keeps interchanging bilaterally between each other [3]. Therefore, intelligence of the exoskeleton system is enhancing while the power of the human operator is also improved. The principal criterion to control the exoskeleton robot, especially power assist exoskeleton robot is to work according to the user motion intention. This becomes much more important for physically weak person who are not capable of generating daily motions properly.

A schematic representation of the 1-DOF lower limb exoskeleton actuated at the knee done in this thesis is shown in figure 3.1. The knee will be driven by a DC servomotor. The motor is connected to the lower part which is intended to support the shank of human. Here the control method used is EMG based.

Briefly the control procedure is described as follows:

1. The position sensor obtains the position of the knee.

2. Position data from the sensor is changed to voltage and compared with the EMG signal. The integrated error is applied to the LQG controller.

3. The rotation of the knee is facilitated by one actuator and thus rotating the lower part of the exoskeleton to the intended position.

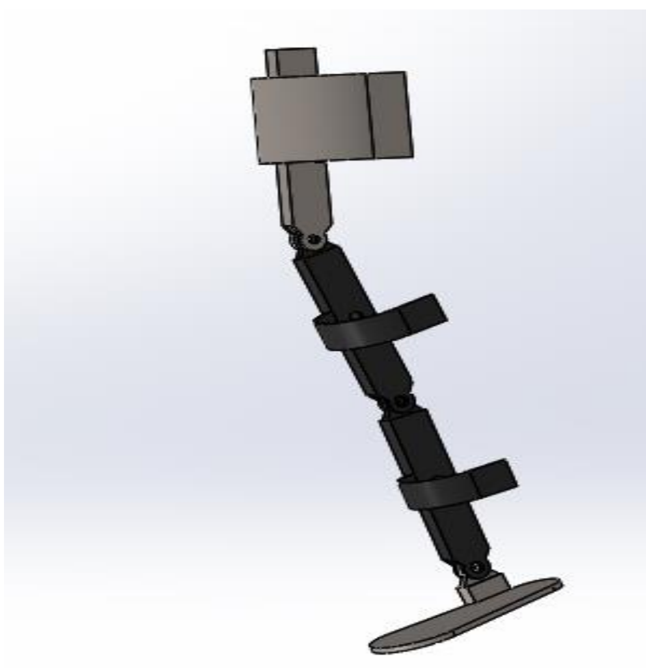

Figure 3.1: 3D design on Solid works

3.1.2. The exoskeleton actuation system

In order to be used for an exoskeleton the drive system should be Lightweight, Small sized, providing enough driving torque, and having good dispersion thermal performance. Choosing the right actuator is critical step in developing robots. The exoskeleton actuation system which are commonly used so far are of three types namely the Electric Motors, the pneumatic system, and the hydraulic system.

Hydraulic actuators uses an incompressible fluid as working medium for energy transfer and controlling transmission modes. Hydraulic actuators are rugged and suited for high-force applications. They can produce forces 25 times greater than pneumatic cylinders of equal size. They also operate in pressures of up to 4,000 psi. Hydraulic motors also have high horsepower-to- weight ratio by 1 to 2 hp/lb greater than a pneumatic motor, can hold force and torque constant without the pump supplying more fluid or pressure due to the incompressibility of fluids, and can have their pumps and motors located a considerable distance away with minimal loss of power. Hydraulics will leak fluid which leads to cleanliness problems and potential damage to surrounding components and areas, require many companion parts; including a fluid reservoir, motors, pumps, noise-reduction equipment etc.; this makes for linear motions systems that are large and difficult to accommodate can be listed among the Limitations of such actuators. The BLEEX series from the University of California and XOS series adopts hydraulic drive.

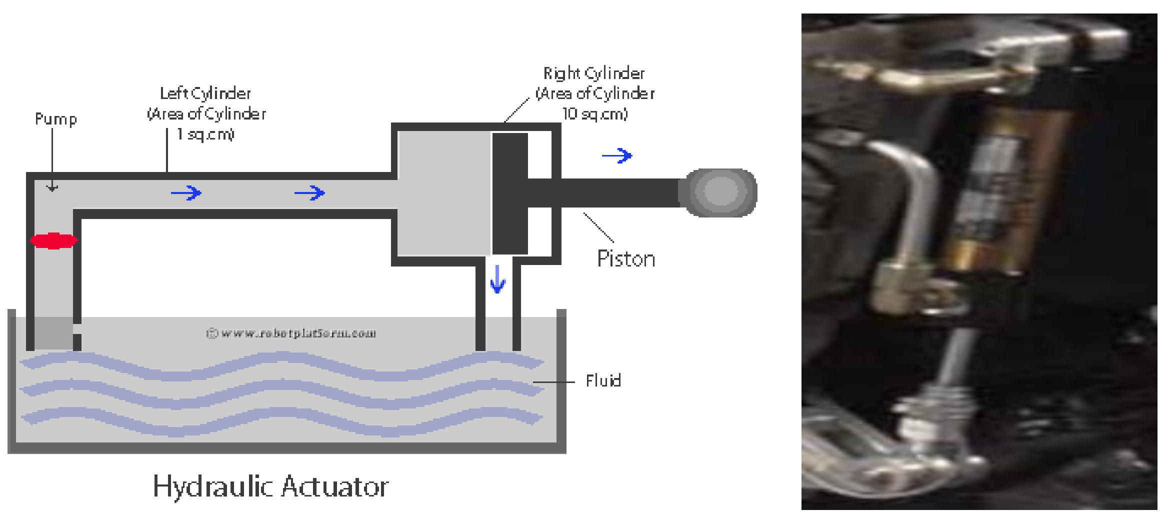

Figure 3.2 Hydraulic actuator (left and) the hydraulic knee actuator used in BLEEX[14]

Pneumatic actuators utilizes compressed air as working medium for energy transfer and controlling the mode of transmission with typical forces ranging from 20 to 4000 pounds. The benefits of Pneumatic actuators come from their simplicity. Most pneumatic aluminum actuators have a maximum pressure rating of 150 psi with bore sizes ranging from 0.5 to 8 in., which translate into approximately 30 to 7,500 lb. of force. Pneumatic actuators generate precise linear motion by providing accuracy. And to mention some of the drawbacks: the stability of pneumatic transmission speed is slow, high maintenance and operational costs, wastes a substantial amount of electricity when compressor is idling or when the pneumatic system is inadequately maintained, resulting in air leaks. The kanagawa type body exoskeleton robot developed power Assist suit (PAS) uses pneumatic transmission device.

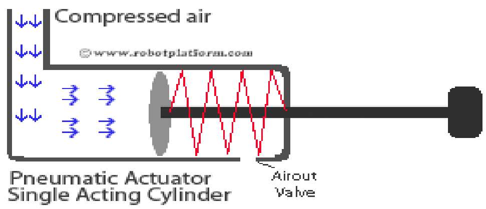

Figure 3.3 Pneumatic actuator

Electric Motors use electric voltage and frequency of the source current equipment as a way of transmission of power and control. Among the advantages of Motor actuator has mature technology, simple structure, no pollution, a wide range of control options for the specific motion profile better adaptability, reduced replacement costs, particularly in applications in which the electronics are separate from the actuator, more flexible drive options, such as using a more economical stepper motor for accurate positioning at lower speeds, or a more costly servomotor for superior performance at high speeds, predictable operating energy costs largely related to motor power draw, low operational costs, quick signal transmission and easy to realize automation. But the Electric motors have big inertia, slow reversing, and mostly needs special driving circuit. The LOPES, HAL series adopt the Electric motor drive technology.

Considering the criteria stated at the beginning of this section DC Servo motor is found to be the best fit for this project. Servo motor is a device of small size with output shaft. Servos are sent a pulse of variable width to control them. They have a bit complex design perhaps this is reason why they are so strong and are popular for various applications. To mention some of its important advantages DC Servo motor has comparatively high power output than the motor weight and size, Encoder sets resolution and accuracy, highly efficient. It can reach up to 90% of light loads, exuberantly high torque to inertia ratio which leads to quick acceleration of loads, reserves power for emergencies and can provide 2-3 times constant power for short time, reserves torque and can provide 5-10 times rated torque for short time, motor remains cool because the current drawn is proportional to load, does not make noise even while running at high speed, and Free of vibration and resonance. And the need to be tuned so as to steady feedback loop, the requirement of service due to the torn out of brush in limited life of about 2,000 hrs, having peak torque fixed to a 1% duty cycle, being damaged by an overload, the need for an encoder can be mentioned among the disadvantages of DC servo motors[32]. Here as we can see the points stated as disadvantage can be corrected or compensated by using the proper control mechanism.

3.1.3. The exoskeleton mechanical structure

As discussed in section 3.1.1 the exoskeleton robot is a kind of machine which is in close contact with the human body, which safety, comfort and practicality should be the factors to be considered first. So the process of designing the mechanical structure of an exoskeleton the range of motion and movement characteristics at the joint should be reasonable as far as possible, should be anthropomorphic, safe and comfortable. The ideal range of motion is from 0° (i.e. straight leg) to 110° (i.e. flexed knee).

3.1.4. Mathematical model

In modeling process, to simplify the analysis and design processes, linear approximations are used as long as the results yield a good approximation to reality[36].

A useful component in many real control systems is a permanent magnet DC servo motor. The input signal to the motor is the armature voltage Va (t), and the output signal is the angular position θ (t). A schematic diagram for the motor is shown in Fig. 3.4. The terms Ra and La are the resistance and inductance of the armature winding in the motor, respectively. The voltage Vb is the back EMF generated internally in the motor by the angular rotation. J is the inertia of the motor and load assumed lumped together), and B is the damping in the motor and load relative to the fixed chassis.

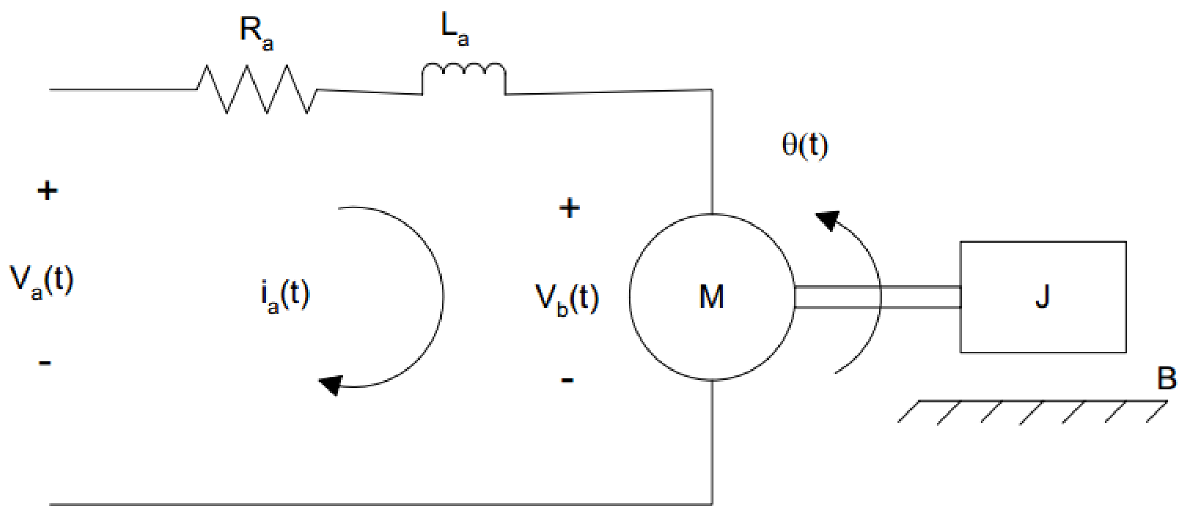

Figure 3.4 Schematic diagram of a DC- servo motor

The equations for the electrical side of the system are

$$V_a\,(t) = R_a i_a(t) + L_a \frac{dia(t)}{dt} + V_b(t) \;\text{ with }\; V_b(t) = K_b \frac{d\theta(t)}{dt}$$

$$V_a(t) = R_a i_a(t) + L_a \frac{dia(t)}{dt} + K_b \frac{d\theta(t)}{dt} \tag{3.1}$$

where Kb is the motor's back EMF constant. The equations for the mechanical side of the system are

$$\frac{Jd^2\theta(t)}{dt^2} + B\frac{d\theta(t)}{dt} = K_t i_a(t) \tag{3.2}$$

where K_t is the torque constant that relates the torque to the armature current.

After Laplace transforming and Defining the state variables, with x_1 being I_a, x_2 being θ, x_3 being dθ/dt , and U being Va, equations 1 and 2 will be re-written as:

$$\dot{x}_1(s) = -\left(\frac{R_a}{L_a}\right)x_1 - \left(\frac{K_b}{L_a}\right)x_3 + \left(\frac{1}{L_a}\right)U$$

$$\dot{x}_2 = x_3$$

$$\dot{x}_2 = \left(\frac{K_t}{J}\right)x_1 - \left(\frac{B}{J}\right)x_3$$

$$y = x_2$$

Hence the state space representation can be given as follows

$$\begin{bmatrix} \dot{x}_1 \\ \dot{x}_2 \\ \dot{x}_3 \end{bmatrix} = \begin{bmatrix} -\frac{R_a}{L_a} & 0 & -\frac{K_b}{L_a} \\ 0 & 0 & 1 \\ \frac{K_t}{J} & 0 & -\frac{B}{J} \end{bmatrix} \begin{bmatrix} x_1 \\ x_2 \\ x_3 \end{bmatrix} + \begin{bmatrix} \frac{1}{L_a} \\ 0 \\ 0 \end{bmatrix} U$$

$$y = [\,0 \quad 1 \quad 0] \begin{bmatrix} x_1 \\ x_2 \\ x_3 \end{bmatrix} \tag{3.3}$$

After obtaining the overall system's state space representation the motor parameters can be selected by either Using system identification techniques on a prototype built or by selecting an actuator based on the requirement of the load torque. Both methods are described next with a clear description of the steps followed.

3.1.4.1 Using system Identification

Among the several approaches to obtain a model of a physical system is to use "system identification" where you input a signals into the plant and observe output signal or the response, and then use these to specify the model that mapped one to the other. Of course, this approach might not lead to a perfect model; however, it is often quite useful since good model information can be obtained from direct experimentation with the plant. Identification of parameters of any physical system plays a vital role to choose the parameters of controllers appropriately. This is essential to make sure that the system controlled satisfies the desired performance specifications.

A prototype was built by the undergraduate team in their study of building an exoskeleton for rehabilitation. As it can be seen in figure 3.5 the prototype was built from an iron arm and a dc servomotor with only the part number, rated voltage, and rated speed was on its nameplate was used as an actuator. Even if the part number of the motor was on the name plate, its datasheet couldn't be available.

Figure 3.5: Exoskeleton prototype built by the undergraduate team, AAIT

Besides the parameters of the DC servomotor the parameters of the robot arm, specifically the damping coefficient and inertia, are also unknown. Therefore both the parameters of the motor and the arm need to be identified. The identification process can be done in two ways discussed in the following paragraphs.

The first method is by using the lumped system, i.e. the motor and the arm attached together. Here, we take a simple, direct and practical approach by using a time-domain based approach and frequency domain based approach for continuous time systems [31].

First the step response of the system is recorded by giving a unit step input into the system. Next by giving sine waves with three different frequency into the DC servo at the input V_{in}, say with frequencies 5, 50, and 500 rad/sec, we measure the output of the tachometer in each case and obtain the plots showing both the sine wave input and the output from the tachometer. Then Plot three points on a Bode magnitude (20log ($|G_w|$) vs. log frequency) and phase plot (degrees vs. log frequency).

Then a straight line approximation, by making use of usual Bode plot techniques, to the points has to be specified (i.e. simply sketch it on the Bode plot for the three points). Keeping in mind that the fall off is 20 dB per decade for high frequencies, the two straight lines can be found first, then considering their intersection point and its relation to the third point. From this, the pole location and the Bode gain (DC gain) can be found. Then, sketch the straight line approximation to the phase plot.

Specify a transfer function that would generate this Bode plot by trial and error. Plot the Bode plot of the transfer function that you found, with the three experimental points on the magnitude and phase plots. Compare the bode plot of the model that we identified with the experimental bode plot and check if it fits well. Then, plot the step response of the transfer function that we found and compare to the step response obtained from the time domain based procedure [31].

The other method is identifying the parameters of the DC servomotor and the moment of inertia and friction coefficient of the arm separately. Parameters of the DC servomotor such as torque constant K_T, back emf constant K_b, armature resistance R_a, armature inductance L_a do not vary with load and hence these values are determined using conventional method. However, moment of inertia J and damping coefficient B vary with respect to load. Once those parameters are identified they are put in to equation 3.3,the equation representing the system dynamics.

DC servomotor used in the prototype has the ratings 20V and 180 rpm.

For the winding resistance use an ohmmeter. For a dc motor measure the resistance between the two armature wires. The resistance can be found by varying the input DC voltage and reading the current using an ammeter. Then dividing V_{dc} by I_{dc} and taking the average of the computed resistance values the winding resistance R_a is found. The recorded data is given in the table below:

Table 3.1: voltage and current data collected to find the armature winding resistance

Vdc(v)	1	1.5	2	2.5	3	3.5	4	4.5	5	5.5	6	6.5	7
Idc(A)	0.25	0.26	0.27	0.28	0.28	0.29	0.3	0.31	0.31	0.31	0.32	0.33	0.34
R (Ω)	4	5.78	7.41	8.93	10.71	12.07	13.33	14.52	16.13	17.74	18.75	19.7	20.59

7.5	8	8.5	9	10	11	12	13	14	15	16	17	18	18.5	19	20
0.35	0.36	0.37	0.38	0.41	0.43	0.45	0.47	0.49	0.52	0.54	0.56	0.58	0.58	0.58	0.6
21.43	22.2	22.97	23.68	24.4	25.6	26.7	27.6	28.6	28.8	29.6	30.4	31.03	31.9	32.76	33.3

$$R_a = \sum_{i=1}^{n} R_i / n \tag{3.4}$$

Where n is the number of data points taken which is 29 in this case and R_i's are the Resistance values at each data points. Hence, R_a = 21.056 ohm

The motor winding resistance can also be directly measured using an ohmmeter and giving

R_a= 2.1 ohm.

To measure the motor inductance use a low voltage ac source to the motor winding. For a dc motor, apply the ac voltage to the armature winding measure the voltage and the current. The impedance of the DC motor phase winding is then [30]:

$$Impedance[ohms] = \frac{phase\ voltage[volts]}{line\ current[amps]} \tag{3.5}$$

$$Impedance = \sqrt{reactance^2 + resistance^2} \tag{3.6}$$

$$Reactance[vars] = \sqrt{impedance^2 - resistance^2} \tag{3.7}$$

Solving the reactance from equation 3.7. Note that the phase resistance was calculated previously. Then the inductance can then be calculated from:

$$Inductance\ [heneries] = \frac{reactance[vars]}{2\pi * frequency} \tag{3.8}$$

where frequency = 50hz

In armature control method, the armature voltage and hence the armature current are varied. Back emf is calculated using the expression

$$E_b = V_a - i_a R_a \tag{3.9}$$

The value of angular speed ω is determined from the value of measured speed N in rpm. Back emf is proportional to speed.

$$E_b = K_b \omega \tag{3.10}$$

The slope of the graph obtained by plotting the variation of back emf E_b against speed ω gives the value of K_b. The mechanical equivalent of electrical power and mechanical power are equal at steady state.

$$\omega T_e = E_b i_a \tag{3.11}$$

Electromagnetic torque T_e is proportional to armature current i_a. Therefore,

$$T_e = K_T i_a \tag{3.12}$$

Where K_T is the torque constant. From equations 3.10, 3.11, and 3.12 it can be obtained that

$$K_b = K_T \tag{3.13}$$

Hence, Torque constant K_T is obtained from the slope of the graph obtained by plotting the variation of E_b against ω. DC servomotor with the ratings as already mentioned above is switched on at no load. The armature voltage and hence the armature current are varied by armature control method and the corresponding values of speed are noted. Values of ω and E_b are calculated at each armature voltage and current. They are tabulated in Table 3.2, it can be found that K_T for the servomotor is 0.887 Nm/A.

Table 3.2: Data collected for the calculation of the constant, K_T

S. No.	V_a (V)	I_a (A)	Speed (rpm)	ω(rad/sec)	E_b(V)	K_T (Nm/A)
1	1.5	0.26	10.3	1.0786	0.954	0.885
2	2.5	0.28	19.9	2.0839	1.912	0.916
3	4	0.3	31.9	3.3406	3.37	1.009
4	5.5	0.31	44.8	4.6914	4.85	1.034
5	7	0.34	59	6.1785	6.286	1.017
6	8.5	0.37	71.9	7.5294	7.723	1.026
7	10	0.41	111.1	11.6344	9.139	0.786
8	11	0.43	119.7	12.535	10.097	0.806
9	12	0.45	129.9	13.6031	11.055	0.813
10	18	0.58	219.2	22.9546	16.782	0.731
11	20	0.6	244.4	25.5935	18.74	0.732

The torque equation of the motor and load arrangement is given by

$$T_e = \frac{Jd\omega}{dt} + B\omega \tag{3.14}$$

where J and B are inertia and friction coefficient of the arrangement respectively. When the speed is constant, the torque equation becomes

$$T_e = B\omega \tag{3.15}$$

From 3.12 and 3.15,

$$B = \frac{K_T i_a}{\omega} \tag{3.16}$$

Where i_a is the armature current measured at steady state for the given load current. Thus B is determined for the given load current using 3.16.

DC servomotor is switched on at no load. The motor is loaded in steps. At each load current, steady state values of armature current and speed are noted. B is determined at each load using equation 3.16.

When the supply to the armature is switched off, motor speed reduces to zero from its steady speed. Hence, the torque equation becomes

$$\frac{Jd\omega}{dt} + B\omega = 0 \tag{3.17}$$

The solution for equation 3.17 is obtained using the steady state speed as the initial value of speed is expressed by

$$\omega = \frac{T_e}{B} e^{-\left(\frac{B}{J}\right)t} \tag{3.18}$$

When t = ج = J/B, mechanical time constant of the motor, the motor speed reduces from steady state speed to 36.8% of steady state speed. The time taken for speed of the motor to reduce from steady state speed to 36.8% of steady state speed gives the mechanical time constant of the motor and load.

From the time constant, the moment of inertia of the motor and load is given by,

$$J = B\tau \tag{3.19}$$

Thus the moment of inertia of motor and load J can be determined by substituting the values of B and mechanical time constant τ in equation 3.19.

DC servomotor is run at no load and two different load currents. Armature current and speed are measured at each load current. Whenever the motor is switched off, speed response is captured on the Digital Storage Oscilloscope. Speed responses are captured at no load and other two load currents. From these responses, time taken (mechanical time constant) for the speed to drop from its steady state initial speed to 36.8% of its steady state initial speed is noted for no load and two different loads. J is determined for each case using equation 3.19.

As discussed above the values of J and B depend on the load connected to the motor. As we can see the DC servomotor is run with and without load. I have performed the test using the exoskeleton as a load since the motor is expected to actuate as much load as the exoskeleton arm. Though the above procedures can easily be performed in our laboratory with available equipment I was not able to complete using this method since the material used to build the arm was an iron which have a heavy weight, hence a higher torque required than the motor's nominal torque value. When the arm is attached to the DC - servomotor the motor draws a higher current above the rated current which holds me from proceeding through the above procedures.

3.1.4.2 Selecting an actuator based on the requirement of the load torque

For an efficient and successful robot it is necessary to look at the various forces that both inhibit and help the operations of a robot. It is important to select the right servo motor for a specific joint as over loading can cause the life of the servo to be cut short[38].

Firstly the maximum torque, which happens where the force applied is perpendicular to the arm, required of the servo will be defined by the force (moment) acting about it.

Moment = Force (Newton) x Distance (Meters).

The force the arm will exert on the servo will be determined by a number of factors. The main consideration is the weight that the arm is required to lift. Secondly the weight and length of the arm are two important factors. The weight of the arm and the weight of the load must be added together. The length of the arm is also important as it determines the distance of the load from the fulcrum (pivot point). As

$$\text{Moment} = \text{Force x Distance},$$

The moment acting around the servo will be greater the longer the arm.

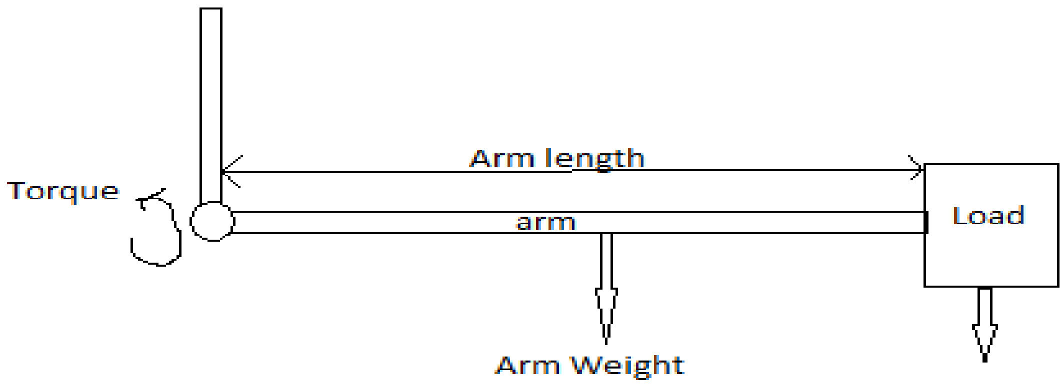

Figure 3.6. Simple schematics of a robot arm used for moment calculation

To calculate the total moments about the servo we should add the moments of the arm and the load together.

$$\text{Moment} = (\text{Load weight x arm length}) + (\text{arm weight} * \tfrac{1}{2} \text{ arm length})$$

Notice that for the arm length we only use half the value. This is because the weight of the arm is acting over the entire arm and not at the very end of it. In this thesis I have taken the center of gravity of the arm is the center of the arm. Once this calculation has been complete the answer is the actual torque being applied.

Table 3.3: Body segment data used in torque calculation

No.	Body segment	Average Value
1	Weight of an African adult[41]	60.7Kg
2	Percentage of total body weight of shank[34]	4.57%
3	Percentage of total body weight of foot [33]	1.33 %
4	Length of human shank (L_{shank}) [34]	44cm

From the table Mass of shank (M_{shank}) = 4.57% of 60.7 Kg = 2.774Kg and

Mass of foot (M_{foot}) =1.33% of 60.7 Kg= 0.807 Kg

Therefore the total mass of the load = $M_{shank} + M_{foot}$

= 2.774+0.807= 3.581 Kg.

And the weight of the load (W_L) = mass of the load * gravitational acceleration

= 3.581 * 9.81 = 35.12961 N

Taking length of the robot arm (L_{arm}) = L_{shank}=44cm and

Mass of the arm (covering from knee to ankle) = 0.7Kg

Weight of the arm = mass of the arm * gravitational acceleration

= 0.7Kg * 9.81 m/s^2 = 6.867 N. From the above formula,

Actual torque being applied = (W_l * L_{arm})+(Warm* ½ L_{arm})

= (35.12961N*0.44m) + (6.867N * 0.22m)

= 16.97 Nm

This is the minimum torque required from a motor. To allow for simple overloading and smooth operation a motor of a higher torque value should be used; this is known as a factor of safety. It is recommended to look for a motor with 20% higher torque than the minimum torque required from the motor [38]. Hence,

Torque of the motor should be = 16.97Nm + (20% of 16.97Nm) ≈ 20 Nm

Looking for a DC-servo motor with this nominal torque value I selected QB03402B whose datasheet is included in Appendix B.

Table 3.4: Parameters of QB03402B

Type	Ra (Ω)	La (mH)	Kt (Nm/A)	Kb(V/rad/s)	J_m (Kgm^2)	B_m(Nm/rpm)
QB03402B	0.31	0.75	0.208	0.208	$1.5 * 10^{-4}$	$1.6 * 10^{-5}$

From the selected motor's datasheet the values tabulated above can be used in equation 3.3 by assuming $J \approx J_m = 1.5 * 10^{-4}$ Kgm^2 and $B \approx B_m = 1.6 * 10^{-5}$ Nm/rpm to give the complete state-space representation of the exoskeleton system shown below:

$$\dot{X} = \begin{bmatrix} -413.3 & 0 & -277.3 \\ 0 & 0 & 1 \\ 1386.67 & 0 & -0.107 \end{bmatrix} x + \begin{bmatrix} 1333.3 \\ 0 \\ 0 \end{bmatrix} U$$

$$Y = [0 \quad 1 \quad 0] x$$

3.2. EMG based control

Electromyogram (EMG) based control is a type of control that uses the skin surface EMG signals to be used as input information for the controller. Surface electromyography (sEMG) is the non–invasive recording of electrical muscle activity that is used to diagnose neuromuscular disorders, among other applications. Muscle fibers are activated by motor neurons and the resulting electrical signals produced by the muscle fibers can be detected by electrodes placed on the surface of the skin. The electromyogram, which is the electrical activity of skeletal muscle, finds useful applications in many fields such as biomechanics, rehabilitation medicine, neurology, gait analysis, exercise physiology, pain management, orthotics, incontinence control, prosthetic device control, even unvoiced speech recognition and man–machine interfaces. EMG signals act as a control signal from the user's muscle to provide feedback and to initiate leg movement. Typically, sEMG is acquired in two stages. The first (electrode–amplifier) stage includes signal transduction/detection and pre–amplification. This stage is placed as close to the skin as possible, generally with the electrodes and the electronic amplification arranged within a single package. The second stage provides further signal conditioning [44].

There are two options to obtain the EMG signal for simulation (Simulated EMG signal): One is using a software tool called simulator which makes use of necessary characteristics like the range of frequency and the amplitude of the signal, and the other is using a look up table prepared by recording common signal characteristics. Both are discussed in detail in the following sections.

3.2.1. Using a simulator software

Muscle contraction and relaxation is controlled by the central nervous system. The nervous system sends a signal through a motor neuron to a grouping of muscle cells, called fibers. That grouping of muscle cells, and the motor neuron that innervates them, is a motor unit - a basic building block of the neuromuscular system, the smallest functional part of muscle tissue. The signal of the motor neuron causes a chemical reaction that changes the membrane potential of muscle fibers. If the threshold potential is reached a motor unit action potential (MUAP) occurs, causing the electrical activation to spread along the entire surface of the muscle fiber at a rate of approximately 3–5 m/s. Electromyography (EMG) is a technique that is used to detect and record MUAPs non–invasively by placing a conductive element (electrode) on the surface of the skin overlying the muscle of interest (this method is referred to as surface EMG) or directly inside the muscle (this invasive EMG detection method utilizes needles or fine wires). Inserted electrodes record from a very small region of muscle, making it possible to view individual MUAPs. On the contrary, surface electrodes tend to record from much larger regions of the muscle. Thus, individual MUAPs are not clearly visible, as many motor units tend to be contracting concurrently. Only the superposition (interference) pattern is recorded. Needle EMG gives access to deep musculature, has higher sensitivity and higher frequency and voltage ranges. Needle electrodes are suitable for detecting changes in motor unit size and internal structure, as well as revealing their abnormal function. Unlike surface EMG, needle EMG can detect action potentials of spontaneously contracting muscle fibers — fibrillation potentials, which are a sign of interruption of the nerve connection to an organ. Surface EMG is better for gathering data on: various aspects of behavior; temporal patterns of activity, or fatigue of the muscle as a whole or of muscle groups; location of the innervation zone; length and orientation of fibers; and highly accurate measurement of muscle–fiber conduction velocity. Surface electrodes are indispensable when needle measurement is not appropriate or measurements need to be made repeatedly. Surface electrodes do not require medical supervision, cause minimal discomfort and are easier to apply than wire electrodes, although they are mainly used on superficial muscles, have limitations with recording dynamic muscle activity and have concerns with crosstalk of adjacent muscles. A needle and surface electrode comparison by Giroux and Lamontagne (1990) revealed no significant differences in either isometric or dynamic muscle contraction detection. However, needle EMG acquisition has several disadvantages that can make use of surface EMG more desirable: detection may not represent an entire muscle while repositioning is nearly impossible; insertion of the needle into the muscle requires sterilization of the instrumentation and the environment; needles are difficult to use on muscles located in sensitive areas, such as muscles in the tongue, lips, and face; there is minor muscle tissue damage, that in turn affects shapes of action potentials; although low, there is a risk of infection; needles might not be suitable for children or persons who poorly tolerate procedures involving use of needles (Groh). The two methods are better suited for a different span of applications and have their own advantages and disadvantages and are therefore both currently used for EMG signal detection [37].

Most sEMG signals have a frequency content ranging from 0 to 500 Hz, with dominant energy between 50 to 150 Hz. However, content at up to 2000 Hz may be useful. The amplitude of the signal may vary from less than 50 μV up to 30 mV (Clancy et al., 2002). The nature of sEMG signals and various EMG equipment properties determine the quality of a recording.

Besides motor unit (muscle cell group) and electrode characteristics, there are other factors that distort and add undesirable noise to the signal. A DC offset due to half–cell potentials within the tissues can be as high as 300 mV. Muscle crosstalk (signals from motor units of neighboring muscles) may result in misleading information about the investigated muscle. Ambient 60 Hz noise from power supplies (50 Hz for European power supplies) may result in power line noise three fold the magnitude of the sEMG itself. Inherent noise generated by electronic equipment can range from zero to thousands of Hz. Motion artifacts due to electrode or cable movement add noise to the EMG signal in the frequency range of 1 to 5 Hz [37].

Hence feeding the above signal characteristics and information like the number of motor units in the muscle, electrode type, needle positions, etc. the EMG signal can be generated from the simulator software.

3.2.2. Using a look up table

A raw EMG signal is a voltage that can be both positive and negative and changes as the neural command calls for increased or decreased muscular effort. It is quite difficult to compare the absolute magnitude of an EMG signal from different muscles because the magnitudes of the signals can vary depending on many factors (e.g. gain of the amplifiers, the types of electrodes, etc.). In order to use the EMG signals in a neuro-musculo-skeletal model, we first need to normalize them into a specific range (between 0 and 1) so that we can eventually compare them one with another.

A look up table prepared by recording common EMG properties that is the amplitude versus the time and normalizing. Some of the normalized amplitude versus time values are shown in the table below [45].

Table 3.5: Some of the EMG data from the look up table used

Amplitude (volts)	-0.0650	-0.0683	-0.0750	-0.0767	-0.0750	0.0200	0.0217	0	0
Time	11.4285	11.4288	11.4292	11.4298	11.4300	11.4593	11.4595	11.4622	11.4625

Amplitude	0.1750	-0.0117	-0.0767	0.0000	0.0633	-0.0100	0.0633	-0.0500	0.0467
Time	11.5190	11.5195	10.0985	9.16425	9.1215	8.96975	7.9045	6.396	5.5735

Amplitude	-0.1733	0.1900	0.0200	-0.0733	-0.0100	0.0433	-0.1117	-0.0433	-0.0333
Time	4.46825	3.4	2.99975	2	1.84625	0.812	0.8	0.159	0.00025

The plot of the obtained emg value is shown in the Figure below

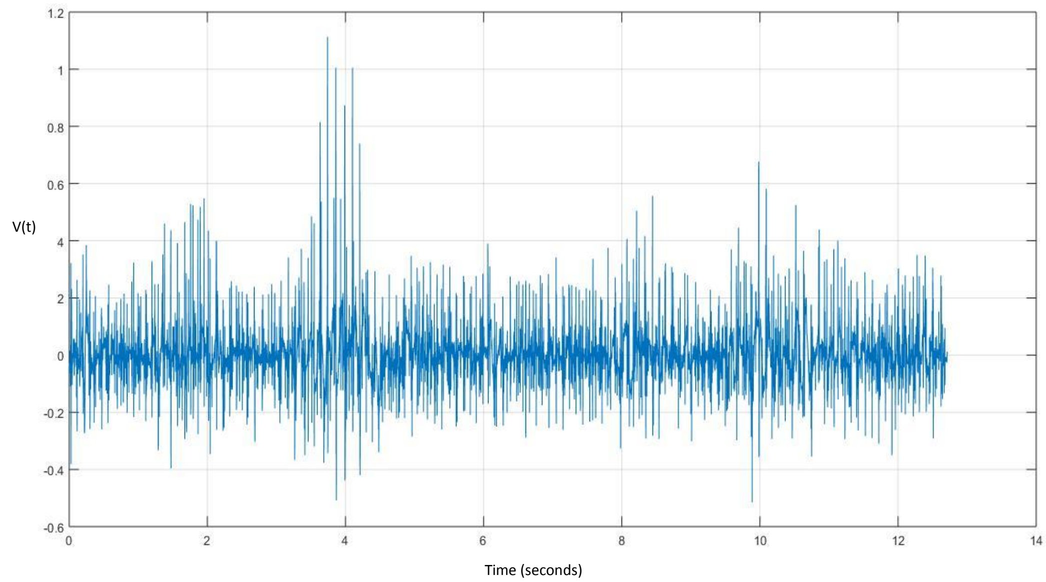

Figure 3.7: The plot of the simulated EMG signal

3.3. Controller Design

3.3.1. Introduction

The accurate control of motion is a fundamental concern in Mechatronics applications, where placing an object in the exact desired location with the exact possible amount of force and torque at the correct exact time is essential for efficient system operation [36].

The first step in control system design is to find an answer on the question: 'which controller will be used'. The answer depends on the specific properties and demands of the system. The system which has to be controlled in this case is the knee of the exoskeleton. The non-linear friction is a dominant property of the system. As mentioned in the objectives description in chapter 1, the main demands of the controller are robustness and gentleness. The system has non-linear parts due to the possible parameter variations and the coulomb friction. A robust controller is needed to handle this behavior. State feedback control, like a PID controller, is an adequate mechanism to control systems with this uncertainty. A possible problem with the PID controller is the differential action (dt /du). The input signal can be noisy and can give problems during differentiation.

A model based controller is also a robust way to control systems with non-linear parts. The LQG controller is a model based controller, which makes estimations of the states to calculate the state feedback control gain. The advantage of a model based controller compared with a classic controller is the digital characteristics and the complete mathematical formulation of the control mechanism.

LQG method is rooted in optimal control theory and in spite of systematic design procedure, shows some useful properties of robustness and good performance. In this method, the desired shapes for singular values of the sensitivity function of the closed- loop plant must be designed in an LQG problem and then these singular values are recovered at the input or output of the real plant by successive tuning of a gain in an LQR problem. The state space equations of the open-loop plant for a standard LQG problem is:

$$\dot{x} = Ax + Bu + Gw$$

$$y = Cx + v$$

Where A,B,C are state space matrices of the plant, G is the disturbance input matrix which is selected equal to B for simplicity, u is control input vector , and y is the output of the plant. w and v are disturbance input and measurement noises , respectively, which are assumed Gaussian noises with zero mean and covariance matrices W and V as follows:

$$E\ \{ww^T\} = W > 0,\ E\ \{vv^T\} = V>0.$$

It is assumed w, v are also that uncorrelated with each other, so

$$E\{wv^T\} = 0.$$

Then the control problem is to find the feedback control law which minimizes the following performance index:

$$J = E\ \left\{ \lim_{T\to\infty} \frac{1}{T} \int_0^T (z^T Q z + u^T R U) dt \right\} \tag{3.20}$$

In the relation shown above in equation 3.20, z is a linear combination of the system states, R and Q are symmetric positive definite and symmetric positive semi-definite weighting matrices, respectively.

Most of the time the weighting matrices Q and R selected to be the covariance matrices W and V respectively, i.e.

$$Q = E\ \{ww^T\}$$

$$\text{and } R = E\ \{vv^T\}$$

The optimal solution of the LQG problem formulated above is obtained based on decomposition principle. According to this principle, the optimal solution of equation 3.20 is achieved by solving two different optimization problems. The first problem is to find the optimal estimate $\hat{x}$ of states of the system x by minimizing the mean square of the state estimation error:

$$J1 = E\ \{(x - \hat{x}\ )^T (x - \hat{x}\ )\} \tag{3.21}$$

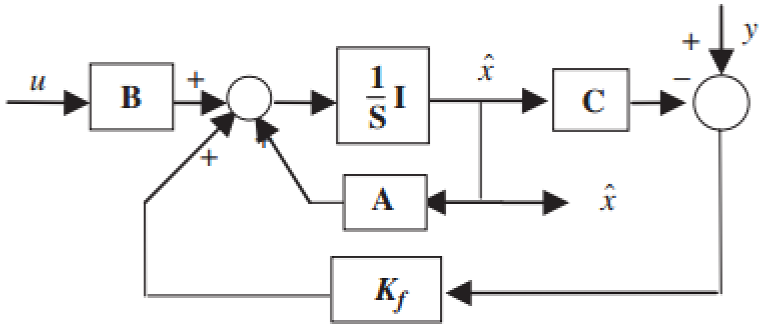

Figure 3.8 Kalman - filter block diagram [35].

This problem is known as Kalman filtering, which is based on probabilistic and measurement noises. The kalman filter is an observer that is used for navigation and other applications that require the reconstruction of the state from noisy measurements. Since it is fundamentally a low-pass filter, it has a good noise rejection capabilities. Its block diagram is depicted in Figure 3.8. Note that the Kalman filter inputs are plant inputs and outputs, and the output is an estimate of state $\hat{x}$. The Kalman filter gain K_f can be obtained by:

$$K_f = P_f C^T R^{-1} \tag{3.22}$$

where Pf is a symmetric positive semi-definite matrix and is the solution of the following Riccati equation:

$$AP_f + P_f A^T + GwG^T - P_f C^T R^T C P_f = 0 \tag{3.23}$$

The solution of this problem which is an estimate of the states of the system will result in an estimate of the z by the following relation:

$$\hat{z} = M\,\hat{x} \tag{3.24}$$

The next problem is to use this estimate to solve a linear quadratic regulator (LQR) problem by minimizing the following performance index:

$$J_2 = \int_0^T (z^T Q z + u^T R u) dt \tag{3.25}$$

Actually, the goal of this method is to divide the original LQG problem in to two easier problems, which are well-known, and their solutions can be obtained easily. The optimal gain Kc in Fig. 2 for this standard LQR problem can be achieved from:

$$K_c = R^{-1} B^T P_c, \tag{3.26}$$

Where P_c is a symmetric positive semi-definite matrix and is the solution of the following Riccati equation:

$$A^T P_c + P_c A - P_c B R^{-1} B^T P_c + M^T Q M = 0 \tag{3.27}$$

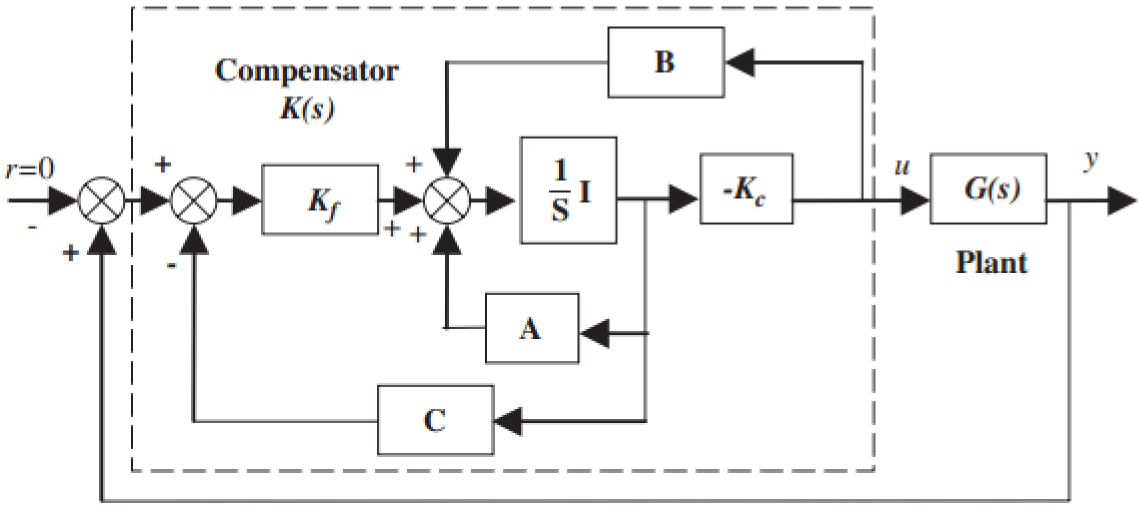

Figure 3.9: Complete Diagram of LQG

The conditions for existence of gains in Eqs. (3.22) and (3.26) and internal stability of closed loop system are that state space realizations (A, B, $Q^{1/2}M$) and (A, $Gw^{1/2}$, C) be stabilizable and detectable, respectively. Notice that both Kalman filter and LQR problems show robust performance and robust stability characteristics [35].

3.3.2. Design of LQG controller

Based on the procedure described in the previous section an LQG controller for the exoskeleton whose model is mentioned in Section 3.1.4 is designed.

Some of the objectives which must be met by closed- loop system are:

1. Because of good command following and disturbance rejection it is required to augment the open-loop system with integral action in each loop.

2. Transient response including overshoot and settling time of the step response are also important and should be remained in a sensible range.

3. Stability and performance of the closed- loop system should be robust with respect to the uncertainty of the plant and actuator dynamics.

3.3.2.1. Design of Kalman filter

As mentioned before, it is assumed the disturbance is acted through the same channel as the control input on the plant. The first step in the design procedure is to have a state estimator, by Kalman filtering.

The Linear Quadratic Estimator mechanism is used when not all states of a system are measurable. In this case the states to be estimated are the armature current, the position of the knee, and the angular velocity of the knee. Before LQE can be used, the 'observability' of the system has to be checked. A system is observable if all states influence the output. Matlab is used to check the observability of the system by using the rank (obsv (A, C)) command. It turns out the system is observable. When the system is observable, the optimal observer can be designed [23].

To estimate the states in an optimal way is to determine the feedback matrix K_f optimal. The K_f matrix can be determined analytically by the use of the covariance matrices Q and R as discussed above. The covariance Q represents the magnitude for the noise on the states and the covariance R represents the measurement noise. For this purpose the covariance matrices of the plant disturbance Q, and the output measurement noise R, are the design parameters and are assumed as white noise sources. The dimension of Q must be square with as many columns as G which is one for our case. The variance P_f in the error equation (3.28) has to be minimized to find the conditions in the course of which the derivation of P_f is zero. These conditions give the optimal value for K_f [35].

$$\dot{e} = Ax + Bu + Gw - A\hat{x} - Bu - K_f\,(Cx + v - c\hat{x})$$

$$= \left(A - K_f C\right)e + Gw - K_f v \tag{3.28}$$

As a first trial these covariance matrices are selected as identity. i.e. Q = 1 and R = 1. Then the MATLAB command [KEST , K_f, P_f] = kalman (sys ,Q ,R ,n) returns the estimator gain K_f and the steady-state error covariance P (solution of the associated Riccati equation).

$$K_f = \begin{bmatrix} -7.7111 \\ 4.8229 \\ 11.6302 \end{bmatrix}$$

$$\text{And } P_f = \begin{bmatrix} 0.2150 & -0.0008 & 0.0001 \\ -0.0008 & 0.0005 & 0.0012 \\ 0.0001 & 0.0012 & 1.0750 \end{bmatrix} * 1.0e+04$$

The Q and R matrices need to be tuned until satisfactory behavior is obtained.

3.3.2.2. Design of LQR

The Linear Quadratic Regulator method can only be used when all the states in the system are influenced by the input signal. The necessary condition for an optimal state feedback system is the controllability. This property will be checked first. MATLAB is used to check the controllability of the knee joint by using the command rank (ctrb (A, B)).The dynamic system of the knee joint is controllable.

The matrix Q is a weight matrix for the system noise, the matrix R for the measurement noise. Both matrices have to be determined manually. The choice for Q and R is a trade-off between control performance (Q large) and low input energy (R large). Only the relative values of Q and R are relevant. The Q and R matrices need to be tuned until satisfactory behavior is obtained.

The basic model of a LQR controlled system is given in Figure 3.10. In this model w(t) is the system noise and v(t) the measurement noise.

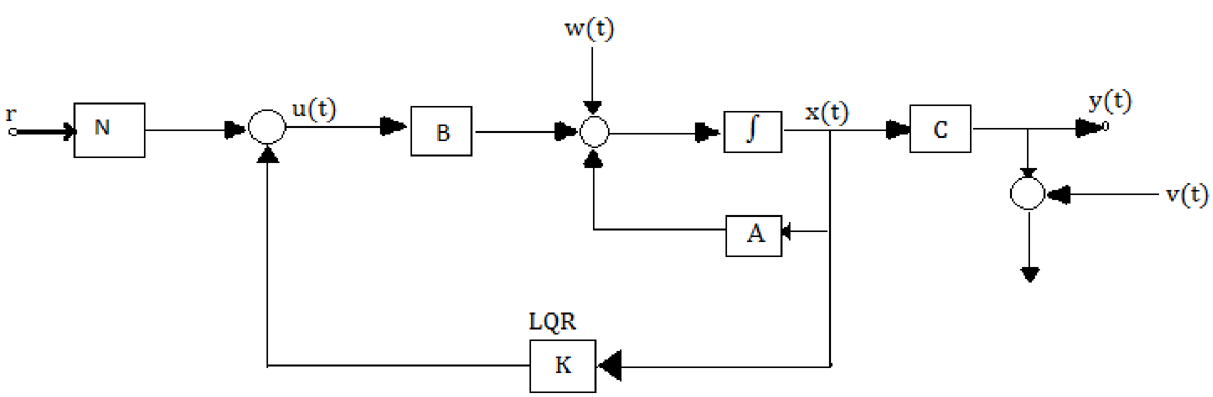

Figure 3.10: Basic model of an LQR controlled system

Similar to the procedure in Kalman estimator design the matrices Q and R for the LQR algorithm are defined first. The optimal magnitude is found by trial and error. The Q and R matrices have to be. The Q matrix is a 3x3 matrix, the dimension of the Q matrix has the same dimension as the A matrix of the system. The dimension of the R matrix is dependent on the amount of outputs of the system (the number of rows of the C matrix). Similarly the matrices Q and R are assumed to be identity at first and are tuned so that an acceptable error appears together with realistic torque commands.

Therefore with

$$Q = \begin{bmatrix} 1 & 0 & 0 \\ 0 & 1 & 0 \\ 0 & 0 & 1 \end{bmatrix}$$

And R= [1]

And using the MATLAB command [K_c, P_c, E] = lqr (SYS, Q, R, N) calculates the optimal gain matrix K_c for a continuous-time state-space model SYS, the state-feedback law u = -Kx minimizes the cost function in equation 3.25 Also returned are the solution S of the associated algebraic Riccati equation and the closed-loop eigenvalues E = EIG(A-B*K).

$$K_c = [\,1.3604 \quad 1.0000 \quad 0.8145],$$

$$P_c = \begin{bmatrix} 0.0010 & 0.0008 & 0.0006 \\ 0.0008 & 1.0226 & 0.0012 \\ 0.0006 & 0.0012 & 0.0012 \end{bmatrix} \text{ and}$$

$$E = \begin{bmatrix} -1.1131 + 0.8058i \\ -1.1131 - 0.8058i \\ -0.0010 + 0.0000i \end{bmatrix} * \ 1.0e + 03$$

Chapter 4. Simulation Result and Discussion

4.1. Introduction

The 3-D model for the lower limb exoskeleton system designed on solid works® is shown in Figure 3.1 in section 3.1.1.

The movement of the part below the knee, containing the support for the shank and the foot, are controlled by signals from the Simulink® model; however, the rotation of the knee is limited.

The complete Simulink® model implemented on MATLAB® is shown in Figure 4.1. The model is used in the study of the frequency response and robustness of the system whose simulation results are given in the next sections.

The interface between the solidworks® model of the lower limb exoskeleton system as shown in Figure 3.1 and the controller to be implemented is shown in Figure 4.2. The solidworks® model is imported to MATLAB using simmechanics® product.

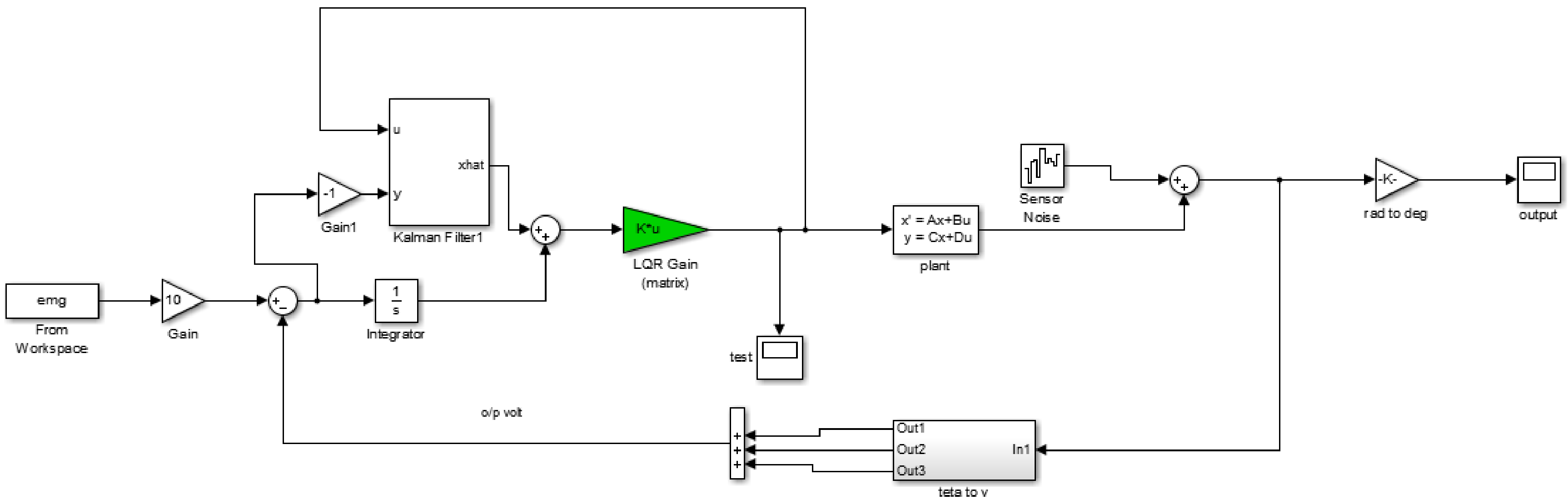

Figure 4.1: Simulink model using the system transfer function model

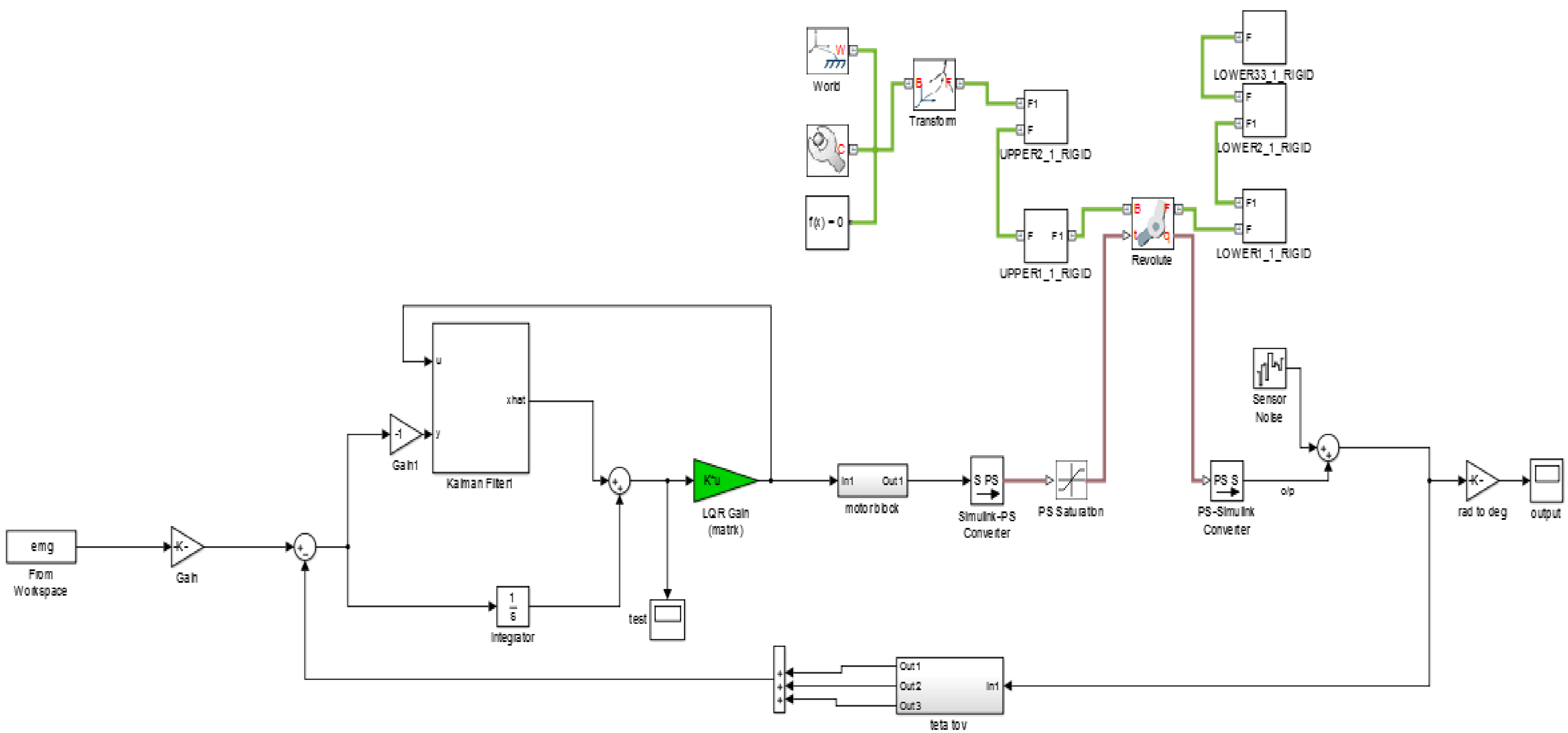

Figure 4.2. Simulink model with the solid works model being imported to MATLAB

The motor block is shown below:

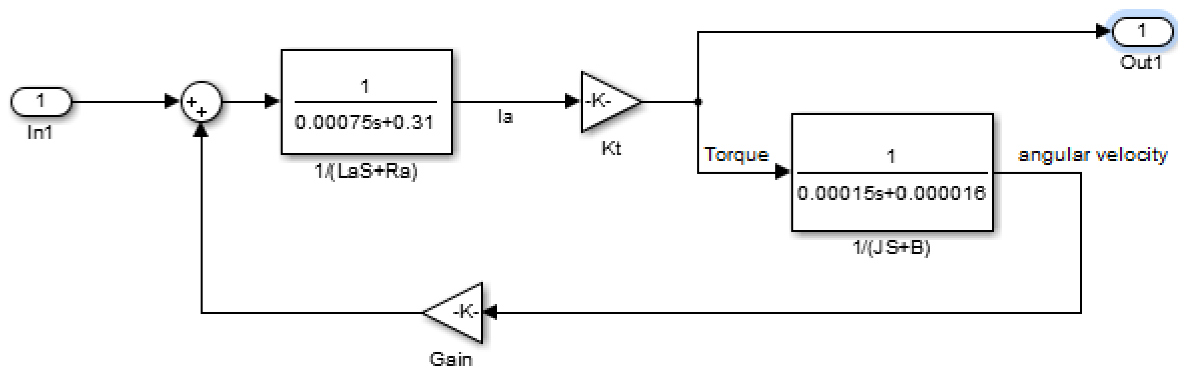

Figure 4.3 DC-servo-motor block diagram representation

4.2. Tuning of the covariance matrices of the plant disturbance Q and the output measurement noise R

As it is indicated in section 3.3 in the course of designing the Kalman state estimator and the linear quadratic regulator we first begin by taking the values of Q and R as unity, or identity matrix as needed, and then by looking at the response on simulation. Hence the necessary and functional controller is found by tuning the parameters Q and R until satisfactory response is obtained. Though the ideal range of motion taken in this thesis is between 0^o and 110^o considering the required motion in everyday life and the safety of the user, the joint motion of the proposed exoskeleton system can be extended to between 0^o and 120^o [4]. Hence in evaluating the results the safe deviation of angle is 10 degrees.

Here the EMG signal from the look up table, whose value is presented in voltage as a function of time, is used as a reference input.

Case I. $Q = \begin{bmatrix} 1 & 0 & 0 \\ 0 & 1 & 0 \\ 0 & 0 & 1 \end{bmatrix}$ and R = 1

The LQR gain matrix becomes k= [1.3604   1.0000   0.8145] and varying the Q and R values of the Kalman filter results in a singularity in the Simulink design. Hence tuning the values of Q and R is mandatory.

Case II. $Q = \begin{bmatrix} 0.01 & 0 & 0 \\ 0 & 0.01 & 0 \\ 0 & 0 & 0.01 \end{bmatrix}$ and R = 10, K= [0.0096   0.0316   0.0024]

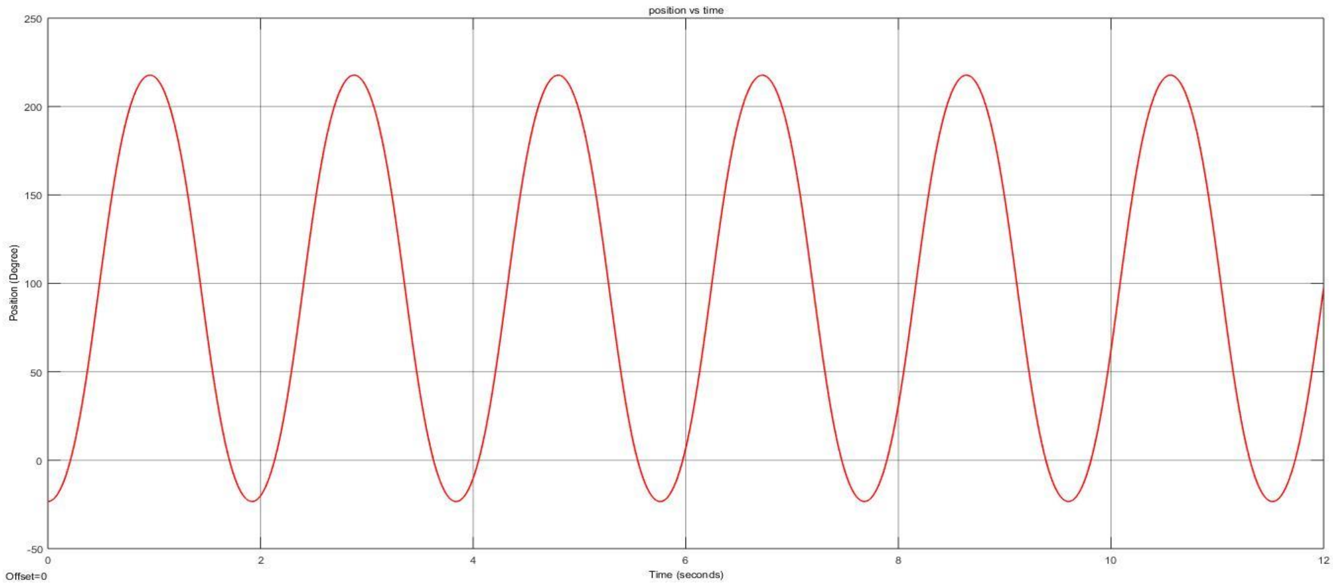

And for the kalman filter using Q = 0.01 and R = 10

Figure 4.4: Result from case II

Case III. $Q = \begin{bmatrix} 0.03 & 0 & 0 \\ 0 & 0.03 & 0 \\ 0 & 0 & 0.03 \end{bmatrix}$ and R=50 gives K= [0.0058 0.0245 0.0015]

Q=0.01, R=50 for the Kalman filter

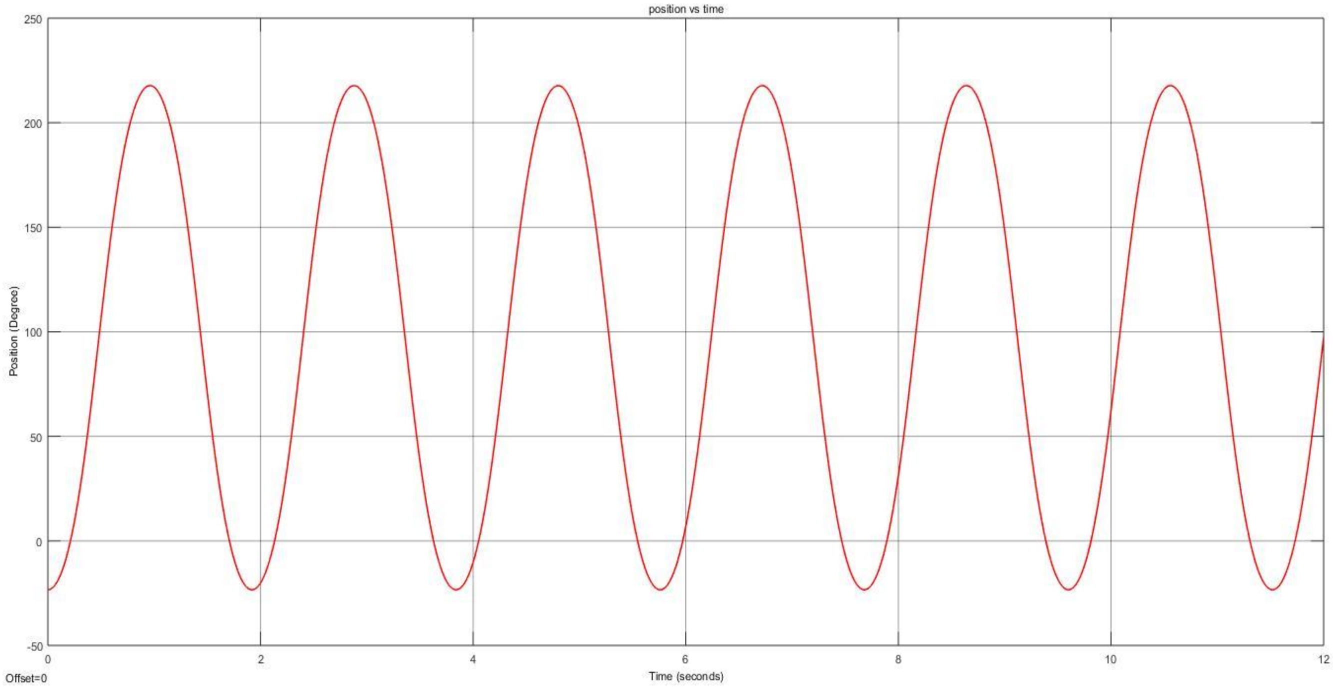

Figure 4.5: Result of case III

As it can be seen in the above cases, case II and case III, the rotation angle is 106 degrees greater than expected, which was 110 degrees. This much angle difference is not tolerable even for a healthy person, hence further tuning is a must.

Case IV. $Q = \begin{bmatrix} 0.001 & 0 & 0 \\ 0 & 0.001 & 0 \\ 0 & 0 & 0.001 \end{bmatrix}$ AND R =50, K = [0.0002 0.0045 0.0001]

Q = 0.01, R = 50

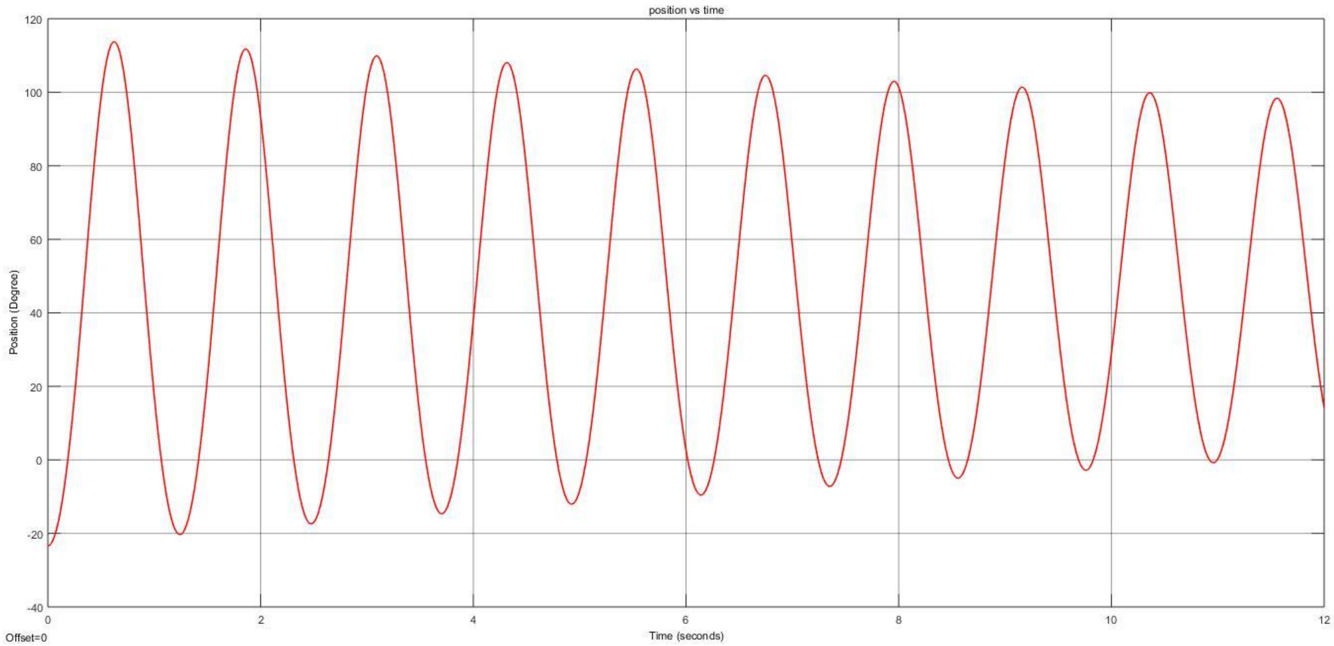

Figure 4.6: Result of case IV

The response from the selection of Q and R parameters in case IV above are much convenient than the previous responses. In recording the rotation angle of the joint we get a maximum value around 113.75 degrees, which have a smaller error or difference from the allowable maximum value (i.e. 3.75 degree) compared to the other values.

Hence the suitable values of Q and R chosen by tuning are:

$Q = \begin{bmatrix} 0.001 & 0 & 0 \\ 0 & 0.001 & 0 \\ 0 & 0 & 0.001 \end{bmatrix}$ and R =50 in LQR design and Q= 0.01 and R = 50 in the Kalman estimator design resulting a maximum overshoot of 3.75 degrees

4.3. Robustness tests

4.3.1. Robustness to sensor noise

A wrong movement at the knee joint level may cause instability. Therefore, an important property of the control law is to regain the intended position whenever an unpredictable flexion or extension occurs. This means that the control law should be robust with respect to external disturbances like sensor noise that may affect the knee joint and consequently the whole stability and safety of the wearer. In the simulation shown above I have tried to add the model of sensor noise/external disturbance.

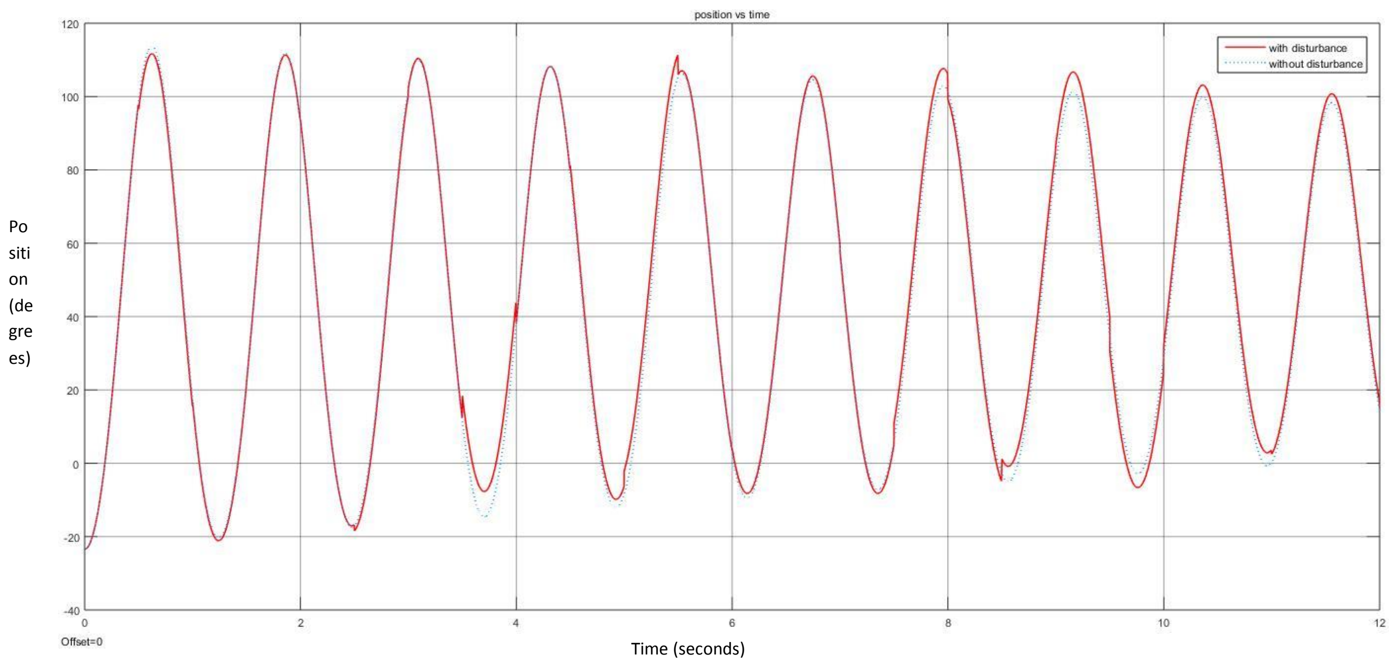

Figure 4.7: Comparison of the response of the system alone and with sensor noise considered

From the response observed the maximum difference between the disturbed and undisturbed system's response is 4.65 degrees and the maximum rotation of the knee joint is found to be 111.66 degrees, that is a maximum overshoot of 1.66 degrees. Therefore we can tell that the system is robust to external disturbance.

4.3.2. Robustness to unmodelled dynamics

In calculating the weight of the load to determine the load torque it can be seen that average weight value for an African adult is used which is 60.7 Kg as taken from literatures. But the fact is that some of the patients might weigh above the average value and some might weigh below. Therefore in testing the developed mechanism the effects of such unmodelled variations in weight should be considered.

Here in the process of testing the robustness of the system to unmodelled dynamics (varying weight) a second generation solid body element is added to the simmechanics block imported as shown in Figure

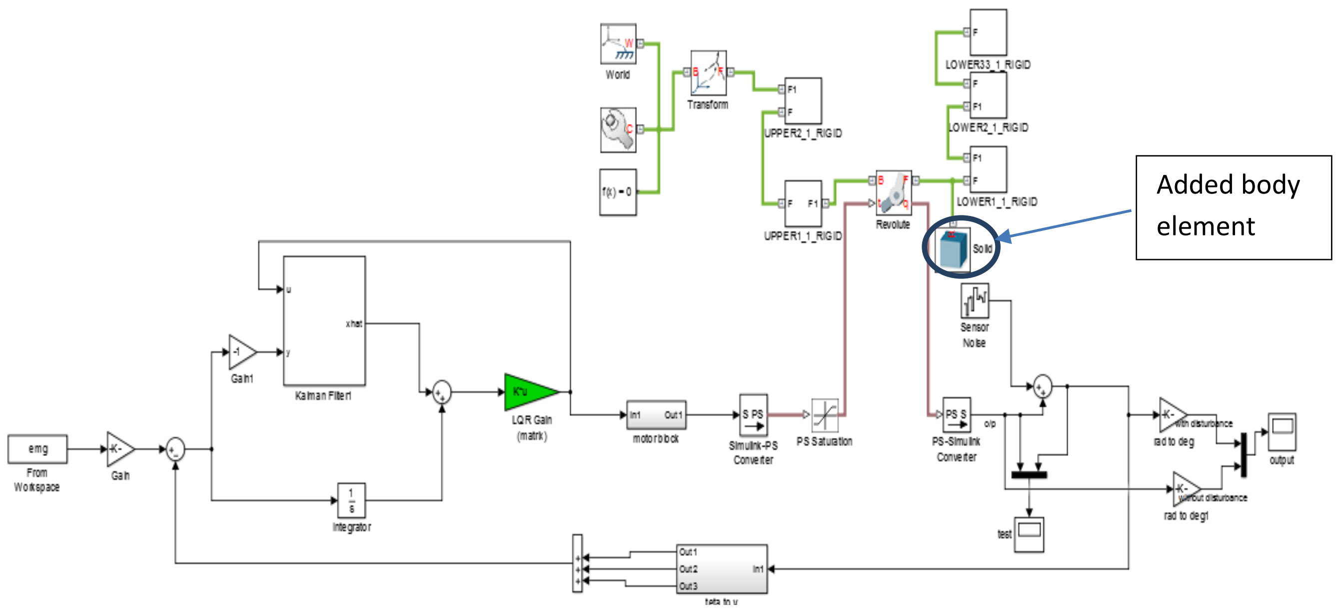

Figure 4.8: A simulation setup to demonstrate robustness to unmodelled dynamics

4.8 below.

Case I. For a patient weighing less than the average value: a weight of 1.6 Kg considered for the weight of the load. A maximum of 113.7305 degrees is recorded which shows only a difference of 3.7305 degrees. This value is tolerable for application on a patient as also showing a smooth swiping animation on the 3D mechanics explorer.

Figure 4.9: Knee joint position with respect to time for an underweight patient

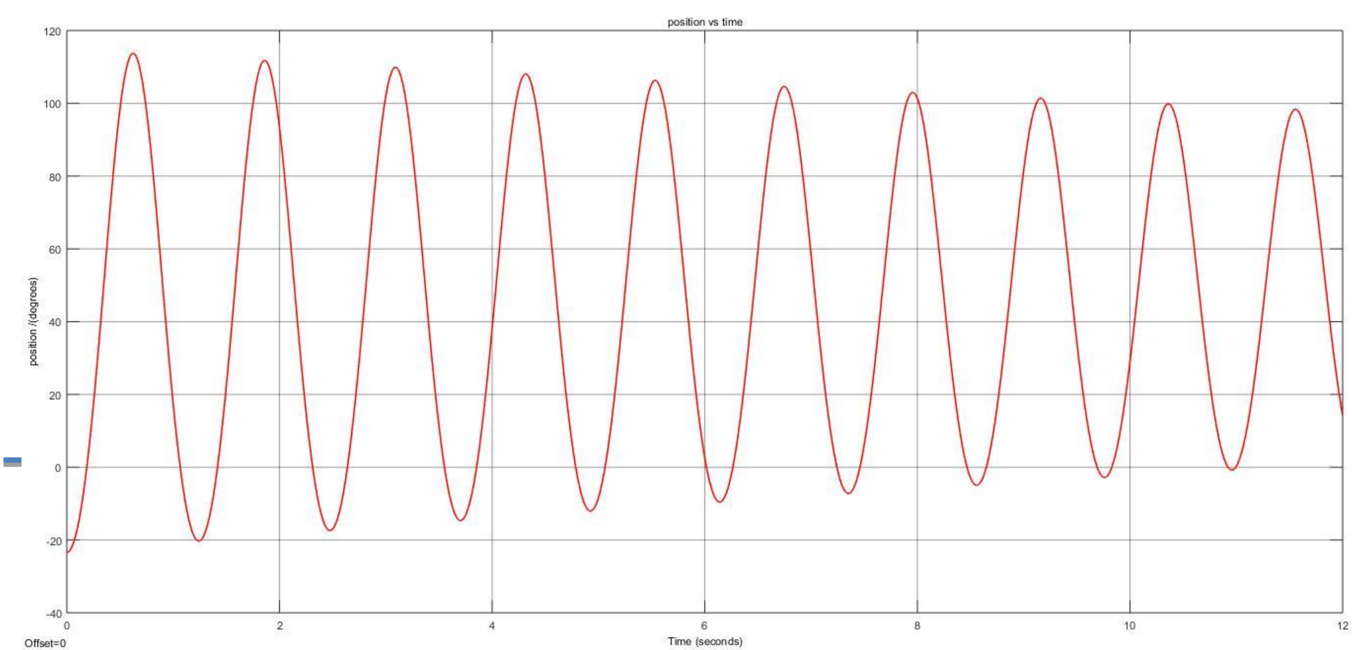

Case II. For a patient weighing above the average value: a weight of 5.5 Kg was taken as the weight of load. As it can be seen in Figure 4.10 the arm is swiping back and forth with a maximum backward rotation of 120 degrees for 9.18 seconds. After 9.18 seconds the arm rotates within the range 53 degrees to 131.185 degrees, resulting with a peak overshoot of 21.185 degrees. For this case we can see that the knee joint will not be fully extended to 0° and the range of motion covered is 78.185 degrees which is

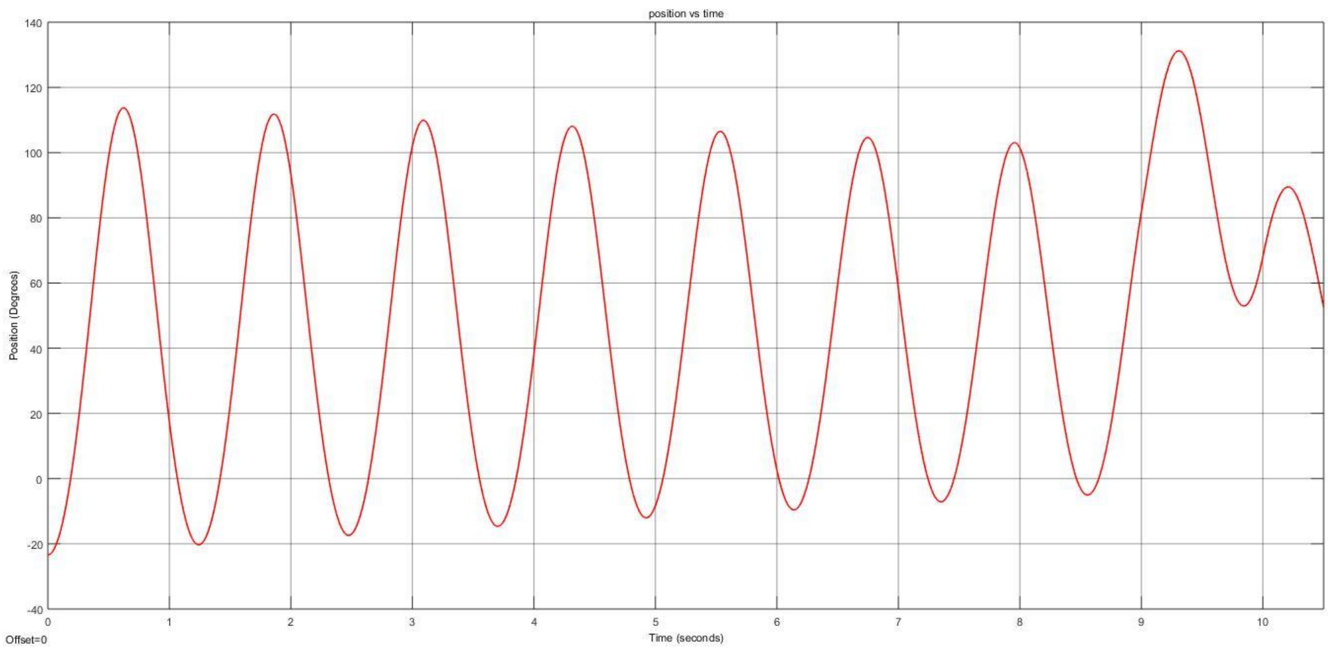

still tolerable compared range of motion allowed to cover, which is 110 degrees.

Figure 4.10: Knee joint position with respect to time for an overweight patient

Chapter 5. Conclusions, Recommendations and Future work

5.1. Conclusion

In this thesis, the dynamic equation representing the lower limb exoskeleton and a linear quadratic Gaussian controller is developed to control the lower limb exoskeleton.

Two models were utilized in this thesis: The first one is mathematical model solved from physical principles and the other one is modeling in 3D CAD models. In mathematically modeling the system two approaches were followed. The first approach modeling using system identification was based on the prototype built by the undergraduate team. Even if not used in this thesis, due to the prototype’s heavy weight than the motor’s capacity, experimental procedures were carried out to obtain some parameters like armature resistance R_a and torque constant K_T. The other approach was by selecting an actuator based on the requirement of the load torque, i.e. looking for a DC-servo motor after finding the maximum torque needed to move the arm.

The other challenge was obtaining a simulated EMG signal and was achieved by the use of a look up table. Once the simulated EMG signal and the model of the lower limb exoskeleton system is obtained the next job was designing the LQG controller. The controller gains are found by tuning the covariance matrices of the plant disturbance Q and the output measurement noise R until satisfactory response is obtained.

In this thesis the results from the solidworks® model is discussed by varying the values of Q and R until suitable response is obtained.

The ideal range of motion is taken in the range from 0° (i.e. straight leg) to 110° (i.e. flexed knee). The performance of the controller is demonstrated using the actual knee joint rotation angle with respect to the desired or the ideal range of motion. The tracking performance is further evaluated by tuning the covariance matrices of the plant disturbance Q and the output measurement noise the knee joint is able to track the ideal range of motion with an error of less than 5 %(less than maximum of 4 degrees difference).

The effect of external disturbance in the performance of the controllers is demonstrated using a band limited white noise of noise power $15*10^{-4}$ and sample time 0.5 second. Even in the presence of disturbance, it is seen that linear quadratic Gaussian (LQG) control yields superior control in the feedback system owing its robustness property.

The other study done was on the robustness of the system to unmodelled dynamics. Here the variation of weight was considered as the parameter resulting in variation of parameters from the modelled dynamics. Since the average weight is considered first the cases for underweighted and over weighted person were investigated. And the result found was satisfactory with a peak overshoot of 3.7305 degrees for an underweighted person and peak overshoot of 21.185 degrees for over weighted person, still assuring the robustness of the designed system.

5.2. Recommendation

In this thesis, the multivariable property of the lower limb exoskeleton system is handled by actuating only the knee and considering the angular position of the knee joint. However, the coupling terms and the nonlinearities which led to the modeling of the system as a single-input single-output (SISO) problem could be considered to investigate the multivariable property of the system.

Additionally solving the singularity issue in the revolute joint, i.e. the knee, could be more advantageous in selecting a more robust controller for the lower limb exoskeleton system.

5.3. Future Work

Although this thesis has successfully accomplished the mission which was targeted, there are other different issues and works to be done with in this subject in the future. Some of them are listed below:

- In this thesis actuation of only the knee is considered but all the joints of a lower limb; the hip, the knee, and the ankle joints; need to be actuated. Hence design of the complete lower limb exoskeleton can be done in the future.
- Using the exact EMG signals rather than the simulated one for a better study of the relationship between the muscle’s intention and the position of the knee joint.
- Carry out a parameter variation research to find out to which extent the controller works acceptably.
- Implementation of the designed system with safety, comfort, and practicality taken in to consideration.
- Extend the application of the system from rehabilitation to give walk assistance.

References

[1] Aaron M. Dollar and Hugh Herr, “Lower Extremity Exoskeletons and Active Orthoses: Challenges and State-of-the-Art”, IEEE TRANSACTIONS ON ROBOTICS, VOL. 24, NO. 1, FEBRUARY 2008.

[2] J.M.P Gunasekara, R.A.R.C Gopura, T.S.S Jayawardane and S.W.H.M.T.D Lalitharathne, “Control Methodologies for Upper Limb Exoskeleton Robots”, IEEE/SICE International Symposium on System Integration, 2012.

[3] Walid Hassani, Samer Mohammed,and Yacine Amirat, “Real-Time EMG driven Lower Limb Actuated Orthosis for Assistance As Needed Movement Strategy”, LISSI Lab, University Paris Est Cr´eteil (UPEC) Vitry Sur Seine, 94400, France.

[4] Kazuo Kiguchi, Takakazu Tanaka, and Toshio Fukuda, “Neuro-Fuzzy Control of a Robotic Exoskeleton With EMG Signals”, IEEE TRANSACTIONS ON FUZZY SYSTEMS, VOL. 12, NO. 4, AUGUST 2004.

[5] Christian Fleischer, “Controlling Exoskeletons with EMG signals and a Biomechanical Body Model”, PHD Dissertation, 2007.

[6] Mohd Azuwan Mat Dzahir and Shin-ichiroh Yamamoto, “Recent Trends in Lower-Limb Robotic Rehabilitation Orthosis: Control Scheme and Strategy for Pneumatic Muscle Actuated Gait Trainers”, January 2014.

[7] D. C. Johnson, D. W. Repperger, and G. Thompson, "Development of a mobility assist for the paralyzed, amputee, and spastic patient," in Biomedical Engineering Conference, 1996., Proceedings of the 1996 Fifteenth Southern, 1996, pp. 67-70.

[8] S. Hesse, C. Bertelt, M. Jahnke, A. Schaffrin, P. Baake, M. Malezic, and K. Mauritz, "Treadmill training with partial body weight support compared with physiotherapy in nonambulatory hemiparetic patients," Stroke, vol. 26, pp. 976-981, 1995.

[9] R. S. Mosher, "Handyman to hardiman," Proc. Automot. Eng. Cong., vol. 67008, p. 1, 1967.

[10] T. B. Sheridan, Telerobotics, automation and human supervisory control: The MIT press, 1992.

[11] Y. Ikeuchi, "Control device for walking assistance device," EP2033612 B1, 2007.

[12] H. K. Jun Ashihara, "Walking Assistance Device," EP2055288 B1, 2007.

[13] K. Yasuhara, "Motion Assist Device," US8287473 B2, 2006

[14] Adam Zoss, H. Kazerooni, Andrew Chu, "Biomechanical design of the Berkeley lower extremity exoskeleton (BLEEX)," Mechatronics, IEEE/ASME Transactions on, vol. 11, pp. 128-138, 2006.

[15] J. F. Jansen, L. Oak Ridge National, E. United States. Dept. of, S. United States. Dept. of Energy. Office of, and I. Technical. Phase I Report DARPA Exoskeleton Program, 2004. Available on http://www.osti.gov/servlets/purl/885609-rrTXDr/

[16] A. Tsukahara, R. Kawanishi, Y. Hasegawa, and Y. Sankai, "Sit-to-Stand and Stand-to-Sit Transfer Support for Complete Paraplegic Patients with Robot Suit HAL," Advanced Robotics, vol. 24, pp. 1615-1638, 2010.

[17] H. Kawamoto and Y. Sankai, "Power assist system HAL-3 for gait disorder person," Computers helping people with special needs, pp. 19-29, 2002.

[18] H. A. Quintero, R. J. Farris, C. Hartigan, I. Clesson, and M. Goldfarb, "A powered lower limb orthosis for providing legged mobility in paraplegic individuals," Topics in spinal cord injury rehabilitation, vol. 17, pp. 25-33, 2011.

[19] A. Goffer, "Gait-locomotor apparatus," ed: Google Patents, 2006.

[20] G. A. Pratt and M. M. Williamson, "Series elastic actuators," in Intelligent Robots and Systems 95.'Human Robot Interaction and Cooperative Robots', Proceedings. IEEE/RSJ International Conference on, pp. 399-406, 1995.

[21] N. Hogan, "Impedance Control: An Approach to Manipulation," in American Control Conference, 1984, pp. 304-313.

[22] L. L. Cai, A. J. Fong, C. K. Otoshi, Y. Liang, J. W. Burdick, R. R. Roy, and V. R. Edgerton, "Implications of assist-as-needed robotic step training after a complete spinal cord injury on intrinsic strategies of motor learning," The Journal of neuroscience, vol. 26, pp. 10564-10568, 2006.

[23] Henk van Twillert, “Modelling of the dynamic system and designing a gentle and robust control system for the knee joint of the gait rehabilitation robot LOPES”, university of Twente, 2005.

[24] D. J. Reinkensmeyer, D. Aoyagi, J. L. Emken, J. A. Galvez, W. Ichinose, G. Kerdanyan, S. Maneekobkunwong, K. Minakata, J. A. Nessler, and R. Weber, "Tools for understanding and optimizing robotic gait training," Journal of rehabilitation research and development, vol. 43, p. 657, 2006.

[25] A. M. Dollar and H. Herr, "Lower extremity exoskeletons and active orthoses: challenges and state-of-the-art," Robotics, IEEE Transactions on, vol. 24, pp. 144-158, 2008.

[26] Shen Bingquan , “Design and Control Methodology of a Lower Extremity Assistive Device”, PHD thesis, National University Of Singapore, 2014.

[27] H. Kawamoto and Y. Sankai, "Comfortable power assist control method for walking aid by HAL-3," in Systems, Man and Cybernetics, 2002 IEEE International Conference on, 2002, p. 6 pp. vol. 4.

[28] J. Rosen, M. Brand, M. B. Fuchs, and M. Arcan, "A myosignal-based powered exoskeleton system," Systems, Man and Cybernetics, Part A: Systems and Humans, IEEE Transactions on, vol. 31, pp. 210-222, 2001.

[29] S. K. Banala, S. K. Agrawal, A. Fattah, V. Krishnamoorthy, W.-L. Hsu, J. Scholz, and K. Rudolph, "Gravity-balancing leg orthosis and its performance evaluation," Robotics, IEEE Transactions on, vol. 22, pp. 1228-1239, 2006.

[30] C.Ganesh, B.Abhi, V.P.Anand, S.Aravind, R.Nandhini and S.K.Patnaik, “DC Position Control System – Determination of Parameters and Significance on System Dynamics”, ACEEE Int. J. on Electrical and Power Engineering, Vol. 03, No. 01, Feb 2012.

[31] Kevin M. Passino and Nicanor Quijano, “Modeling and System Identification for a DC Servo”, The Ohio State University, 2004.

[32] Harrie Dadhwal, “How Dc Servo Motors Can Be Advantageous and Disadvantageous”, available on- http://www.selfgrowth.com/articles/how-dc-servo-motors-can-be-advantageous-and-disadvantageous/, July 13,2015.

[33] Paolo de Leva, “Adjustments to Zatsiorsky-Seluyanov's Segment Inertia Parameters” Journal of Biomechanics 29 (9), pp. 1223-1230, 1996.

[34] Plagenhoef, S., Evans, F.G. and Abdelnour, T., “Anatomical data for analyzing human motion” Research Quarterly for Exercise and Sport 54, 169-178, 1983.

[35] J. Zarei, A. Montazeri, M. Reza, J. Motlagh, J. Poshtan, “Design and comparison of LQG/LTR and H_∞ controllers for a VSTOL flight control system”, Journal of the Franklin Institute 344 (2007) 577 – 594.

[36] Farhan A. Salem, “Modeling, Simulation and Control Issues for a Robot ARM; Education and Research”, I.J. Intelligent Systems and Applications, 2014, 04, 26-39.

[37] Marzhan Mozhanova, “Design of a High–Resolution Surface Electromyogram (EMG) Conditioning Circuit”, BSc thesis at Worcester Polytechnic Institute, 2012.

[38] “Applied control technology- Introduction to robotics”, Galway Education Centre.

[39] Roland S. Burns, “Advanced control engineering”, Butterworth-Heinemann, 2001.

[40] Frank L. Lewis, Draguna Vrabie, Vassilis L. Syrmos , “Optimal Control”, second edition, 1995.

[41] Walpole, Sarah C; Prieto-Merino, David; Edwards, Phil; Cleland, John; Stevens, Gretchen; Roberts, Ian; et al. (18 June 2012). "The weight of nations: an estimation of adult human biomass". BMC Public Health (BMC Public Health, 2012.

[42] http://www.stanford.edu/partner/ prosthetics-center-ethiopia, January, 2015

[43] http://www.cheshireservicesethiopia.org/ , January, 2015.

[44] http://www.hopkinsmedicine.org/healthlibrary/test_procedures/neurological/electromyography_emg_92, p07656, February 25, 2016.

[45] http://www.mathworks.com/matlabcentral/answers/249042-how-to-generate-an-emg-signal, February, 2016.

Appendix

Appendix A: Body segment data

Mean Segment Weights

Percentages of Total Body Weight

Segment	Males	Females	Average
Head	8.26	8.2	8.23
Whole Trunk	55.1	53.2	54.15
Thorax	20.1	17.02	18.56
Abdomen	13.06	12.24	12.65
Pelvis	13.66	15.96	14.81
Total Arm	5.7	4.97	5.335
Upper Arm	3.25	2.9	3.075
Forearm	1.87	1.57	1.72
Hand	0.65	0.5	0.575
Forearm & Hand	2.52	2.07	2.295
Total Leg	16.68	18.43	17.555
Thigh	10.5	11.75	11.125
Leg	4.75	5.35	5.05
Foot	1.43	1.33	1.38
Leg & Foot	6.18	6.68	6.43

Plagenhoef et al., 1983

Percentages of Total Body Weight

Segment	Males	Females	Average
Head & Neck	6.94	6.68	6.81
Trunk	43.46	42.58	43.02
Upper Arm	2.71	2.55	2.63
Forearm	1.62	1.38	1.5
Hand	0.61	0.56	0.585
Thigh	14.16	14.78	14.47
Shank	4.33	4.81	4.57
Foot	1.37	1.29	1.33

de Leva, 1996

Mean Segment Lengths

Percentages of Total Body Height

Segment	Males	Females	Average
Head and Neck	10.75	10.75	10.75
Whole Trunk	30	29	29.5
Thorax	12.7	12.7	12.7
Abdomen	8.1	8.1	8.1
Pelvis	9.3	9.3	9.3
Upper Arm	17.2	17.3	17.25
Forearm	15.7	16	15.85
Hand	5.75	5.75	5.75
Thigh	23.2	24.9	24.05
Leg	24.7	25.7	25.2
Foot	4.25	4.25	4.25
Biacromial	24.5	20	22.25
Bi-iliac	11.3	12	11.65

Plagenhoef et al., 1983

Segment Points:

Segment	Proximal	Distal
Head & Neck	Vertex	Mid-shoulder (C7)
Trunk	Mid-shoulder (C7)	Hip
Upper Arm	Shoulder	Elbow
Forearm	Elbow	Wrist
Hand	Wrist	Finger Tip
Thigh	Hip	Knee
Shank	Knee	Ankle
Foot	Heel	Toe

de Leva, 1996

Average weight around the world by region

Table i: ***Average weight around the world by region***

Region	Adult population (millions)	Average weight (Kg)
Africa	535	60.7
Asia	2,815	57.7
Europe	606	70.8
Latin America and the Caribbean	386	67.9
North America	263	80.7
Oceania	24	74.1
World	4,630	62.0

Appendix B: Datasheet of QB3402/03 servomotor

Model No.		**QB03402**			**QB03403**		
Stall Torque (continuous)	oz-in	328			429		
	Nm	2.32			3.03		
Motor Constant	oz-in/√W	44.7			52.8		
	Nm/√W	0.316			0.369		
Elect. Time Constant	ms	2.78			2.37		
Mech. Time Constant	ms	1.57			1.53		
Thermal Resistance	°C/W	1.15			0.92		
Viscous Damping	oz-in/RPM	2.3E-3			3.2E-3		
	Nm/RPM	1.6E-5			2.2E-5		
Cogging Torque (max.)	oz-in	6.5			8.0		
	Nm	0.046			0.056		
Motor Inertia	oz-in-s²	2.2E-2			3.0E-2		
	kg-m²	1.5E-4			2.1E-4		
Motor Weight	oz	61.2			81.0		
	kg	1.73			2.29		
Poles	-	6					
Winding Constants		**A**	**B**	**C**	**A**	**B**	**C**
Design Voltage	V	24	40	130	24	40	130
Peak Torque	oz-in	2090	2307	2307	2516	2961	2961
	Nm	14.7	16.2	16.2	17.7	21.1	21.1
Peak Current	A	91	81	51	96	100	74
Torque Constant (±10%)	oz-in/A	22.9	28.2	45.0	26.0	29.4	39.6
	Nm/A	0.162	0.200	0.318	0.184	0.208	0.280
No Load Speed	RPM	1413	1913	3802	1244	1835	4430
	rad/s	148	200	408	130	192	464
BEMF Constant (±10%)	V/kRPM	16.9	20.9	33.3	19.2	21.7	29.3
	V/rad/s	0.162	0.200	0.318	0.184	0.208	0.280
Terminal Resistance (±12%)	Ohm	0.26	0.40	1.03	0.24	0.31	0.56
Terminal Inductance (±30%)	mH	0.73	1.11	2.82	0.59	0.75	1.36

Appendix C: Internal structure of the Kalman filter block